

Aristotle University of Thessaloniki  
Faculty of Science  
Department of Physics  
Section of Astrophysics, Astronomy  
and Mechanics  
Laboratory of Astronomy



Diploma Thesis:

# Photometric Observations of Asteroids

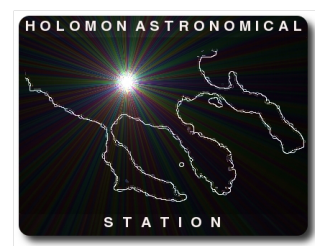
Rotation periods of five large main belt asteroids  
(40km-160km)

**Aikaterini Stergiopoulou**

*Supervisors:*

Professor John H. Seiradakis,  
Assistant Professor Kleomenis Tsiganis

With data from  
**Holomon  
Astronomical  
Station**



Thessaloniki, July 2014

*in Memory of Kiriakos Stergiopoulos,  
my beloved father*

## Acknowledgements

I would like to thank Professor John H. Seiradakis, supervisor of the observational part of this thesis, for his constant interest in the progress of observations and for his encouragement throughout the course of this thesis. I would also like to thank Assistant Professor Kleomenis Tsiganis, supervisor of the theoretical part of the thesis, for his advice and guidance whenever was needed.

I would like to offer my special thanks to my former fellow students Chrysa Avdellidou and Panagiotis Ioannidis who helped me with the technical aspects of CCD photometry and asteroid observations at the beginning.

I wish to thank my family for their support both financial and psychological.

Finally, I want to thank my fellow student and partner, Nikos Iakovidis, for literally standing by me during the observations.

## ΠΕΡΙΛΗΨΗ

Από τη μελέτη των αστεροειδών της κύριας ζώνης αποκτούμε γνώσεις για την εξέλιξη του ηλιακού μας συστήματος. Από τη δομή τους, την κατανομή τους στην κύρια ζώνη, τον σχηματισμό τους και γενικά την εξέλιξη τους μπορούμε να κατανοήσουμε καλύτερα τη διαδικασία σχηματισμού των πλανητών. Η ανάπτυξη της φωτομετρίας με CCD κάμερες τις τελευταίες δεκαετίες έχει οδηγήσει στην απόκτηση μεγάλου αριθμού δεδομένων για τις περιόδους περιστροφής χιλιάδων αστεροειδών. Η σύνθεση καμπύλων φωτός για έναν αστεροειδή από διαφορετικές φάσεις του είναι μια διαδικασία που μπορεί να διαρκέσει χρόνια, αλλά οδηγεί στον προσδιορισμό της διεύθυνσης του άξονα περιστροφής του αστεροειδή και στην κατασκευή μοντέλων για το σχήμα του. Σκοπός της εργασίας ήταν η παρατήρηση αστεροειδών της κύριας ζώνης με CCD κάμερες και η κατασκευή των καμπύλων φωτός τους καθώς και η επιβεβαίωση της (γνωστής) περιόδου περιστροφής τους. Συγκεκριμένα, πραγματοποιήθηκαν παρατηρήσεις των αστεροειδών (354) Eleonora, (213) Lillaea, (79) Eurynome, (374) Burgundia και (173) Ino, οι οποίοι έχουν διάμετρο  $> 40\text{km}$ . Από τις παρατηρήσεις προέκυψαν ολόκληρες οι καμπύλες φωτός ή τμήματά τους. Οι παρατηρήσεις πραγματοποιήθηκαν στον Αστρονομικό Σταθμό του Αριστοτελείου Πανεπιστημίου Θεσσαλονίκης, ο οποίος βρίσκεται στον Χολομώντα Χαλκιδικής.

## Abstract

The study of the main asteroid belt provides us with information about the evolution of the Solar System. Observational data of the physical nature, distribution, formation and evolution of asteroids improve our understanding of the planet formation process. During the last decades a large amount of lightcurves for thousands of asteroids have been collected and their rotation periods were calculated due to development of CCD photometry. Obtaining several lightcurves for a single asteroid at different apparitions can take years, however it results in determining the direction of its spin axis and also in constructing shape models. The aim of this diploma thesis was to obtain the lightcurves of a few main belt asteroids. The MPO Canopus software was used for the analysis of the images with the differential photometry technique. Specifically, the asteroids that were observed are (354) Eleonora for two nights, (213) Lilaea for three nights, (79) Eurynome for one night, (374) Burgundia for three nights and (173) Ino for six nights, all of which have a diameter greater than 40 km. The observations were conducted at Aristotle University's Astronomical Station at Mt. Holomon in Chalkidiki.

# Contents

<b>1</b>	<b>Main belt Asteroids</b>	<b>13</b>
1.1	Formation . . . . .	13
1.2	Discovery . . . . .	13
1.3	Kirkwood gaps . . . . .	15
1.4	Asteroid Orbits . . . . .	17
1.5	Composition of asteroids . . . . .	20
1.6	Main belt asteroid Families . . . . .	21
1.7	Binaries . . . . .	23
1.8	Yarkovsky and YORP effects . . . . .	23
<b>2</b>	<b>Studying Asteroids</b>	<b>25</b>
2.1	Space missions . . . . .	25
2.2	Spectroscopy . . . . .	27
2.3	The study of meteorites . . . . .	27
2.4	Radar observations . . . . .	29
2.5	Photometric observations . . . . .	29
2.5.1	Asteroid rotation . . . . .	29
2.5.2	Size dependence of the rotation rates . . . . .	31
2.5.3	Asteroid rotation period and Lightcurves . . . . .	34
<b>3</b>	<b>Observations and instrumentation</b>	<b>36</b>
3.1	Holomon Astronomical Station . . . . .	36
3.2	Observation dates and equipment used . . . . .	36
3.3	Target selection . . . . .	37
<b>4</b>	<b>Results for asteroids 354 Eleonora, 79 Eurynome, 213 Lilaea, 374 Burgundia and 173 Ino</b>	<b>41</b>
4.1	354 Eleonora . . . . .	41
4.2	79 Eurynome . . . . .	46
4.3	213 Lilaea . . . . .	50
4.4	374 Burgundia . . . . .	55
4.5	173 Ino . . . . .	61
4.5.1	173 Ino <i>phase</i> = 20°.8 . . . . .	62
4.5.2	173 Ino near opposition . . . . .	66
<b>5</b>	<b>Conclusions</b>	<b>71</b>

## List of Figures

1	433 Eros. The picture is a combination of 4 photos taken from NEAR Shoemaker probe. . . . .	15
2	An a-e diagram in which we can see the Kirkwood gaps. The catalog of proper elements of 384,336 asteroids from the AstDys-2 URL: <a href="http://hamilton.dm.unipi.it/astdys2/propsynth/numb.syn">http://hamilton.dm.unipi.it/astdys2/propsynth/numb.syn</a> was used for the construction of the diagram. . . . .	17
3	The orbit plane of a celestial object (in this case of an asteroid) with respect to a plane of reference (in this case to the ecliptic) and the orbital elements. . . . .	19
4	Asteroid families . . . . .	22
5	243 Ida and its moon Dactyl. . . . .	23
6	A diagram of period vs diameter. The rotation periods can be found on the URL: <a href="http://www.minorplanetcenter.net/iau/lists/LightcurveDat.html">http://www.minorplanetcenter.net/iau/lists/LightcurveDat.html</a> and the diameters on <a href="http://vizier.u-strasbg.fr/viz-bin/VizieR-4">http://vizier.u-strasbg.fr/viz-bin/VizieR-4</a> . . . . .	32
7	An a-e diagram in which we can see the asteroids with known period . . . . .	33
8	An histogram for asteroids with diameter $D > 40\text{Km}$ . A sample of 668 asteroids has been used. Slow rotators ( $P > 27\text{h}$ ) have been excluded. . . . .	34
9	The five observed asteroids in an a-e diagram . . . . .	39
10	The five observed asteroids in an a-sinI diagram . . . . .	40
11	Shape model of 354 Eleonora (DAMIT = Database of Asteroid Models from Inversion Techniques) . . . . .	43
12	Raw data 2012/08/05 . . . . .	43
13	Raw data 2012/08/07 . . . . .	44
14	354 Eleonora lightcurve . . . . .	45
15	Shape model of 79 Eurynome (1) (DAMIT) . . . . .	47
16	Shape model of 79 Eurynome (2) (DAMIT) . . . . .	47
17	Raw data 2012/10/01 . . . . .	48
18	79 Eurynome lightcurve . . . . .	49
19	Raw data 2013/04/28 . . . . .	51
20	Raw data 2013/04/29 . . . . .	52
21	Raw data 2013/05/02 . . . . .	53
22	213 Lilaea lightcurve . . . . .	54
23	Raw data 2013/08/08 . . . . .	56

24	Raw data 2013/08/09 . . . . .	57
25	Raw data 2013/08/10a . . . . .	58
26	Raw data 2013/08/10b . . . . .	59
27	374 Burgundia lightcurve . . . . .	60
28	Raw data 2013/04/29 . . . . .	62
29	Raw data 2013/05/02 . . . . .	63
30	Raw data 2013/05/04 . . . . .	64
31	173 Ino lightcurve (ph.) . . . . .	65
32	Raw data 2013/07/25 . . . . .	66
33	Raw data 2013/07/26 . . . . .	67
34	Raw data 2013/07/27 . . . . .	68
35	Raw data 2013/07/28 . . . . .	69
36	173 Ino lightcurve (opp.) . . . . .	70

## List of Tables

1	Prominent resonances of main asteroid belt . . . . .	16
2	Orbital elements . . . . .	18
3	Prominent Main asteroid belt families . . . . .	22
4	Telescopes used . . . . .	36
5	CCD cameras used . . . . .	37
6	Targets and observations dates . . . . .	37
7	Diameters in Km of the five targets . . . . .	38
8	Ephemeris for the observed asteroids . . . . .	41
9	Orbital elements of 354 Eleonora . . . . .	42
10	Orbital elements of 79 Eurynome . . . . .	46
11	Orbital elements of 213 Lilaea . . . . .	50
12	Orbital elements of 374 Burgundia . . . . .	55
13	Orbital elements of 173 Ino . . . . .	61
14	Studied asteroids . . . . .	71

## ΣΥΝΟΨΙΣ

Η πτυχιακή αυτή εργασία ξεκίνησε τον Αύγουστο του 2012, όταν πραγματοποιήθηκαν οι πρώτες παρατηρήσεις του αστεροειδή 354 Eleonora στον Αστρονομικό Σταθμό του Αριστοτελείου Πανεπιστημίου Θεσσαλονίκης στον Χολομώντα Χαλκιδικής. Η εργασία αποτελείται από πέντε κεφάλαια.

Το πρώτο κεφάλαιο περιγράφει την ανακάλυψη του πρώτου αντικειμένου της κύριας ζώνης αστεροειδών το 1801 από τον Guiseppe Piazzi που ονομάστηκε (1) Ceres και πως οι αστρονόμοι της εποχής έψαχναν για έναν πλανήτη που έπρεπε να βρίσκεται σε απόσταση 2.8 Αστρονομικών Μονάδων από τον Ήλιο λόγω του νόμου των Titius-Bode. Έπειτα ακολουθεί περιγραφή των διάκενων Kirkwood. Πρόκειται για κενά στην κατανομή των μεγάλων ημιάξονων των τροχιών των αστεροειδών, η ύπαρξη των οποίων οφείλεται στη βαρυτική επίδραση του Δία. Στη συνέχεια ορίζονται τα έξι στοιχεία που χαρακτηρίζουν την τροχιά ενός αστεροειδή:  $a$ , ο μεγάλος ημιάξονας της ελλειπτικής τροχιάς του,  $e$ , η εκκεντρότητα της τροχιάς του,  $i$  η γωνία που σχηματίζει το επίπεδο της τροχιάς του αστεροειδή με το επίπεδο της εκλειπτικής,  $\Omega$ , ο αναβιβάζων σύνδεσμος,  $\omega$ , η γωνία μεταξύ του αναβιβάζοντος συνδέσμου και του περιηλίου μετρούμενη στη διεύθυνση της κίνησης και  $M$  η μέση ανωμαλία. Επίσης δίνεται το εύρος τους για τους αστεροειδείς της κύριας ζώνης. Τέλος γίνεται μια σύντομη αναφορά στα υλικά από τα οποία μπορεί να αποτελείται ένας αστεροειδής και ο τρόπος ταξινόμησης τους, στην κατάταξη των αστεροειδών σε οικογένειες με βάση τα στοιχεία των τροχιών τους, στις πρόσφατες ανακαλύψεις διπλών και τριπλών συστημάτων αστεροειδών, όπως για παράδειγμα ο αστεροειδής 243 Ida και ο δορυφόρος του Dactyl καθώς και στα φαινόμενα Yarkovsky και YORP και στον τρόπο που επιδρούν στην τροχιά και την περιστροφή των αστεροειδών αντίστοιχα.

Στο δεύτερο κεφάλαιο παρουσιάζονται καποιοι από τους τρόπους με τους οποίους μελετούνται οι αστεροειδείς. Αρχικά αναφέρονται αρκετές διαστημικές αποστολές, όπως οι *Dawn* (NASA), *Galileo* (NASA), *Rosetta* (ESA). Ένας άλλος τρόπος μελέτης αστεροειδών είναι η φασματοσκοπία, με τη χρήση της οποίας επιτυγχάνεται η απόκτηση πληροφοριών για τη σύσταση της επιφάνειας των αστεροειδών. Κατόπιν τονίζεται η σημασία της μελέτης των μετεωριτών διότι μέσω αυτής μελετούμε εμμέσως τη σύσταση των αστεροειδών. Μια άλλη μέθοδος μελέτης αστεροειδών, η οποία είναι σχετικά πρόσφατη, είναι η χρήση ραδιοτηλεσκοπίων και μας δίνει πληροφορίες σχετικά με τα μεγέθη και τα σχήματά τους. Το τελευταίο υποκεφάλαιο ξεκινά με την περιστροφή των αστεροει-

δών. Στη συνέχεια παρουσιάζεται η σχέση των περιόδων αστεροειδών με τη διάμετρο τους καθώς κι ένα διάγραμμα περιόδων περιστροφής σε ώρες και διαμέτρου σε χιλιόμετρα από δείγμα 1279 αστεροειδών. Γίνεται αναφορά στην κατανομή Maxwell που ακολουθεί η περιστροφή αστεροειδών με διάμετρο μεγαλύτερη των 40 χιλιομέτρων και παρουσιάζεται ένα ιστόγραμμα από δείγμα 668 αστεροειδών με διάμετρο μεγαλύτερη των 40 χιλιομέτρων και περίοδο περιστροφής μικρότερη των 27 ωρών. Κατόπιν, αναλύεται η σημασία των φωτομετρικών παρατηρήσεων όχι μόνο για τον προσδιορισμό της περιόδου περιστροφής των αστεροειδών αλλά και για την εύρεση του προσανατολισμού του άξονα περιστροφής τους από συνδυασμό πολλών καμπύλων φωτός.

Στο τρίτο κεφάλαιο δίνονται πληροφορίες (γεωγραφικό πλάτος και μήκος, υψόμετρο) για τον Αστρονομικό Σταθμό στον Χολομώντα Χαλκιδικής όπου έγιναν οι παρατηρήσεις. Περιγράφεται λεπτομερώς ο εξοπλισμός που χρησιμοποιήθηκε. Δύο Schmidt-Cassegrain τηλεσκόπια με διαμέτρους 10 και 11in, δύο CCD cameras και δύο ισημερινές στηρίξεις γερμανικού τύπου. Ο χειρισμός των CCD cameras και των στηρίξεων έγινε μέσω του λογισμικού MaxIm DL, ενώ η επεξεργασία των φωτογραφιών πραγματοποιήθηκε με το λογισμικό MPO Canopus. Οι ημερομηνίες των παρατηρήσεων παρουσιάζονται σε έναν πίνακα καθώς και τι εξοπλισμός χρησιμοποιήθηκε σε κάθε ημερομηνία. Κατόπιν περιγράφεται η διαδικασία της επιλογής στόχων. Τέλος, δίνεται ένας πίνακας με τους στόχους που επιλέχθηκαν και τις διαμέτρους τους, καθώς και δύο διαγράμματα, μεγάλος ημιάξονας-εκκεντρότητα ( $a - e$ ) και μεγάλος ημιάξονας-ημίτονο της κλίσης της τροχιάς ως προς της εκλειπτική ( $a - \sin I$ ), στα οποία ξεχωρίζουν οι επιλεγμένοι στόχοι σε σχέση με ένα δείγμα 384336 αστεροειδών.

Στο τέταρτο κεφάλαιο παρουσιάζονται όλα τα αποτελέσματα. Αρχικά δίνεται ένας πίνακας με τα στοιχεία της τροχιάς για κάθε αστεροειδή, οι εκλειπτικές συντεταγμένες του άξονα περιστροφής και μοντέλο για το σχήμα του από το DAMIT (Database of Asteroids Models from Inversion Techniques) για όσους υπάρχουν και στη συνέχεια ακολουθούν τα δεδομένα για κάθε παρατήρηση και η καμπύλη φωτός που τα συνδυάζει για την εύρεση της περιόδου περιστροφής.

Ο αστεροειδής 354 Eleonora παρατηρήθηκε για δύο νύχτες κι η περίοδος που προέκυψε είναι  $P = 4.277 \pm 0.0017h$ , αποτέλεσμα που συμπίπτει με τα δημοσιευμένα αποτελέσματα. Η διάμετρος του είναι 155.17 χιλιόμετρα και έχει μελετηθεί εκτενώς από 1954 κι έπειτα. Η απόσταση του από τον Ήλιο είναι 2.79868 Αστρονομικές Μονάδες και η κλίση του επίπεδου της τροχιάς του ως προς την εκλειπτική είναι  $18.398^\circ$ , τιμή που

θεωρείται μεγάλη για αστεροειδείς της κύριας ζώνης.

Ο αστεροειδής 79 Eurynome παρατηρήθηκε μόνο για μία νύχτα κι έτσι δεν καλύφθηκε ολόκληρη η περίοδος του. Όμως επειδή λείπει μόνο ένα μικρό κομμάτι παρατηρήσεων της περιστροφής του, η απόπειρα για την εύρεση της περιόδου δεν αποκλίνει σημαντικά από τη δημοσιευμένη τιμή. Η απόσταση του από τον Ήλιο είναι 2.44401 Αστρονομικές Μονάδες και η διάμετρος του είναι 66.47 χιλιόμετρα. Για τον αστεροειδή αυτόν υπάρχουν δύο ζεύγη εκλειπτικών συντεταγμένων ( $\lambda$ ,  $\beta$ ).

Ο αστεροειδής 213 Lilaea παρατηρήθηκε για τρεις νύχτες. Και από αυτήν την καμπύλη φωτός λείπει ένα μικρό κομμάτι παρατηρήσεων, αφενός γιατί η περίοδος του ήταν μεγαλύτερη από αυτήν των προηγούμενων δύο κι επομένως χρειαζόταν περισσότερες ώρες παρατήρησης και αφετέρου γιατί οι παρατηρήσεις αλληλεπικαλύπτονταν που σημαίνει ότι γινόταν παρατήρηση των ίδιων περιοχών του αστεροειδή. Η περίοδος που προέκυψε παρ' όλα αυτά,  $P = 8.034 \pm 0.004\text{h}$ , πλησιάζει πολύ τη δημοσιεύμενη τιμή  $P = 8.045\text{h}$ . Ο αστεροειδής αυτός απέχει από τον Ήλιο 2.75284 Αστρονομικές Μονάδες και η διάμετρος του είναι 83.01 χιλιόμετρα.

Ο αστεροειδής 374 Burgundia παρατηρήθηκε για τρεις νύχτες και προέκυψε ολόκληρη η καμπύλη περιστροφής με περίοδο  $P = 6.969 \pm 0.001\text{h}$ . Απέχει 2.77895 Αστρονομικές Μονάδες από τον Ήλιο και είναι ο μικρότερος σε διαστάσεις στόχος που επιλέχθηκε, με διάμετρο 44.67 χιλιόμετρα. Η καταγεγραμμένη περίοδος για τον αστεροειδή αυτόν είναι  $P = 6.972\text{h}$

Τέλος ο αστεροειδής 173 Ino παρατηρήθηκε για επτά νύχτες, όμως τη μία από αυτές ο αστεροειδής πέρασε μπροστά από έναν αστέρα (occultation) κι έτσι τα δεδομένα αυτά δε μπόρεσαν να χρησιμοποιηθούν στη σύνθεση της καμπύλης φωτός. Τις δύο από τις νύχτες παρατήρησης ο αστεροειδής βρισκόταν σε φάση 20.8 μοιρών, δηλαδή η γωνία Ήλιου-αστεροειδή-Γης ήταν 20.8 μοίρες, ενώ τις υπόλοιπες τέσσερις βρισκόταν σε φάση 7.8 μοιρών. Οι δύο ομάδες παρατηρήσεων συνδυάστηκαν ξεχωριστά λόγω της μεγάλης διαφοράς τους στη φάση και προέκυψαν δύο καμπύλες. Παρά τον μεγάλο αριθμό δεδομένων και τη μικρή σχετικά περίοδο του, ένα κομμάτι παρατηρήσεων λείπει από την καμπύλη λόγω της αλληλεπικάλυψης των παρατηρήσεων. Η περίοδος που υπολογίστηκε από την ομάδα μετρήσεων με τις περισσότερες παρατηρήσεις (4 νύχτες) είναι  $P = 6.111 \pm 0.005\text{h}$ . Ο αστεροειδής αυτός απέχει 2.74366 Αστρονομικές Μονάδες από τον Ήλιο η διάμετρος του είναι 154.10 χιλιόμετρα. Παρατηρούμε ότι στις περιπτώσεις που δεν έχει καλυφθεί παρατηρησιακά ολόκληρη η καμπύλη, μπορούμε να κάνουμε μια εκτίμηση για την τιμή

της περιόδου περιστροφής, δε γνωρίζουμε όμως την ολοκληρωμένη μορφή της καμπύλης φωτός.

Στο τελευταίο κεφάλαιο παρουσιάζονται συγκεντρωτικά τα αποτελέσματα για τις περιόδους περιστροφής καθώς και ένας συγκριτικός πίνακας με τις προϋπάρχουσες τιμές των περιόδων.

# 1 Main belt Asteroids

## 1.1 Formation

In the solar system besides the Sun, the planets, the satellites and the comets there are celestial bodies that are called minor planets or small solar system bodies. Minor planets consist of dwarf planets, main belt asteroids, Trojans, Centaurs and Trans-Neptunian Objects (objects beyond Neptune's orbit).

About 4 and 1/2 billion years ago, a cloud of gas and dust was disturbed and collapsed in on itself (maybe by the shockwave from a nearby supernova which also would have added heavy elements to the collapsing nebula). Density and temperature of the central region reached the point where nuclear reactions began and the Sun was born. The rest of the material circled onto a disk around the new-born Sun. Centimeter and then meter-sized bodies were formed by material accumulation and gentle collisions. These small bodies increased in size by gravitationally attracting other material. Computer simulations by Stuart J. Weidenschilling and the Cosmic Dust Agglomeration Experiment (CODAG) on the Space Shuttle Discovery run by Jurgen Blum and colleagues support this process for the planet and asteroid formation. Close to the Sun, because the temperature was high and most of the icy material was evaporated and blown outwards, the four inner rocky planets were formed: Mercury, Venus, Earth and Mars, from dust grains, while further out from the Sun the gas giants were formed: Jupiter, Saturn, Uranus and Neptune from dust, ice and gas.

The physical nature, distribution, formation and evolution of asteroids are fundamental to our understanding of how planet formation occurred. Main belt asteroids are located between the orbits of Mars and Jupiter, they look like rocks and have irregular shapes with diameter range from meters to hundreds of kilometers. The larger bodies were able to differentiate to form an iron core with a surrounding rocky mantle and crust. Asteroids formed extremely quickly, as recent observations by a team of scientists led by the University of Maryland show. Their research has identified three asteroids with an age of 4.55 billion years.

## 1.2 Discovery

The year 1776, Johann Titius discovered a mathematical formula that described the distances of planets from the Sun. Titius observed that if we add

the number 4 to the number sequence 0, 3, 6, 12, 24, 48, 96 and 192 and then divide each number by 10 the result is the sequence 0.4, 0.7, 1, 1.6, 2.8, 5.2, 10 and 19.6. He realised that this sequence represents the distance of the planets in astronomical units (AU). The numbers 2.8 and 19.6 did not represent none of the known planets. The formula for the distance of the six then known planets was:

$$d = 0.4 + 0.3 \times 2^i, \quad \text{where} \quad i = -\infty, 0, 1, 2, 4, 5$$

Johann Titius published this law in a german translation of a french scientific book, but the law became popular when Johann Bode published it in 1772 and thus this sequence become known as the Titius-Bode law. Now we know that the sequeunce does not have any physical significance.

After the disovcovery of Uranus by Herschel in 1781, it was found that the semi-major axis of its orbit is 19.2 AU which is very close to the number 19.6 predicted from Titius-Bode law. After that, astronomers began to search for the missing planet at 2.8AU.

Xavier von Zach had been searching for the missing planet for 15 years but he did not find anything. He even organised a team to search for it, but the planet was not found. On January 1, 1801, Guiseppe Piazzi who supervised the compilation of the Palermo Catalogue of stars, discovered an object at the right distance of the Sun. This object was named Ceres, after the agriculture goddess.

The discovery of Ceres was followed by the discoveries of many objects that orbit the Sun between Mars and Jupiter. These objects looked like stars because their disk was too faint to be detected with the telescopes existing then and thus they were seen as point sources. This is the reason why they were named asteroids on 1802.

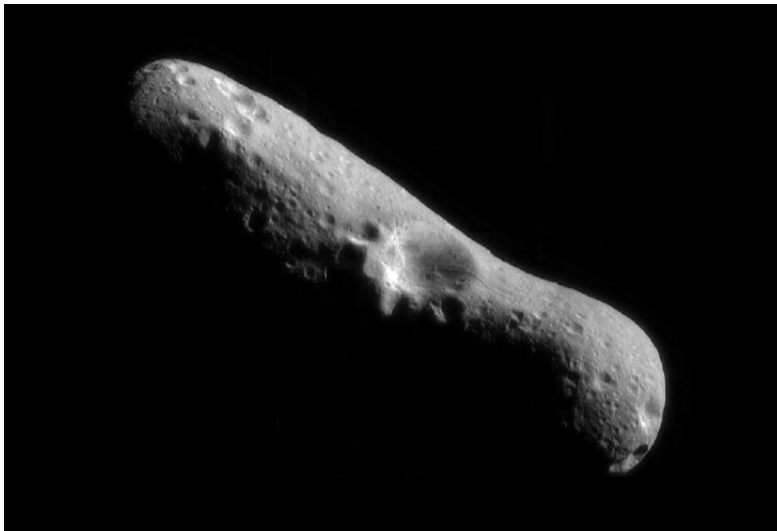
The semi-major axis distribution of asteroid orbits has some empty regions which are called *Kirkwood gaps*. These gaps are the result of the gravitational force of Jupiter. That is also the reason why no other planet was created at this region, between Mars and Jupiter.

Some of the asteroids have orbits with very large eccentricity hence they cross one or more of the planets orbits. Scientists study these asteroids (especially Earth-crossers) because they might crush onto a planet.

Near-Earth asteroids (NEAs) are all near-Earth Objects with no cometary characteristics, with diameter greater than 50m and with orbits that are close to Earth. A potentially hazardous object (PHO) is a near-Earth asteroid or

comet with an orbit such that it has the potential to make close approaches to the Earth and is of a size large enough to cause significant regional damage in the event of impact. One of the largest NEAs is 433 Eros, which is also a Mars-crosser, with size approximately  $33 \times 13 \times 13 \times \text{Km}$ . NEAR Shoemaker probe visited Eros twice, first with a 1998 flyby, and then by orbiting it on February 14, 2000, when it extensively photographed its surface. The photos showed a large number of rocks with diameter greater than 1.2m and also impact craters.

Figure 1: 433 Eros. The picture is a combination of 4 photos taken from NEAR Shoemaker probe.



### 1.3 Kirkwood gaps

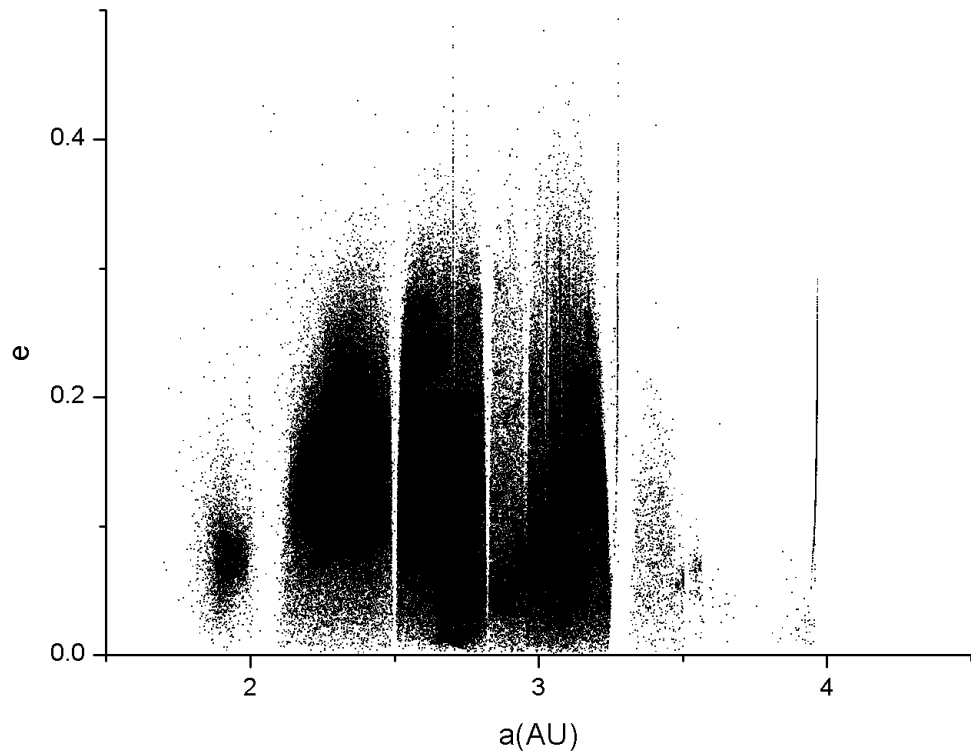
In 1866, Daniel Kirkwood was the first one to notice that there were some gaps in the semi-major axis distribution of main belt asteroids, using a sample of less than 100 asteroids. These gaps correspond to the location of orbital resonances with Jupiter. Resonance is a simple numerical relationship between orbital periods or/and rotation periods of celestial objects. The periods could correspond to one object like the resonance of rotation period and orbital period of the moon around the earth or to orbital (or/and rotation)

period of two or more objects. Resonances occur due to periodic gravitational influence between celestial bodies. The resonances of some prominent Kirkwood gaps are 4:1, 3:1, 5:2, 2:1. On the following diagram which shows the eccentricity ( $e$ ) with respect to the semi-major axis of the main belt asteroid orbits ( $a$ ) in Astronomical Units (Fig. 2), Kirkwood gaps can be seen. We can easily observe gaps at the distances 2.06AU, 2.5AU, 2.82AU, 2.95AU and 3.27AU. For example, by applying Kepler's third law for the orbits with  $\alpha = 3.27AU$ , we calculate the orbital period  $T_a = 5.9132$  years. We know that the orbital period of Jupiter is  $T_j = 11.8626$  years. Thus, the resonance corresponding to the gap that begins at 3.27AU is 2:1, which means that an asteroid with  $\alpha = 3.27AU$  completes two orbits while Jupiter completes one. The two bodies will always be in conjunction in the same region of the asteroid's orbit so that the perturbation by Jupiter at closest approach will always be modifying the asteroid orbit in the same way. The period of the asteroid will change until the asteroid and Jupiter are out of resonance. Kirkwood gaps are not completely empty, but they contain a small number of asteroids. Beyond 3.5 AU, resonances keep asteroids in their present orbits instead of pushing them into different paths.

Table 1: Prominent resonances of main asteroid belt

$\alpha(AU)$	Resonance
2.06	4:1
2.50	3:1
2.82	5:2
2.95	7:3
3.27	2:1

Figure 2: An a-e diagram in which we can see the Kirkwood gaps. The catalog of proper elements of 384,336 asteroids from the AstDys-2 URL: <http://hamilton.dm.unipi.it/astdys2/propsynth/numb.syn> was used for the construction of the diagram.



## 1.4 Asteroid Orbits

The orbit of an asteroid is the path that the asteroid follows around the Sun. Asteroid orbits are ellipses with the Sun located at one of their foci. The closest point to the Sun is called perihelion ( $q$ ) and the furthest aphelion ( $Q$ ). The perihelion and aphelion are calculated by the following equations:

$$q = a(1 - e)$$

and

$$Q = \alpha(1 + e)$$

where  $\alpha$  is the semi-major axis and  $e$  the eccentricity of the ellipse. The orbit of an asteroid is defined by six numbers (orbital elements) plus the epoch for which these numbers are valid.

Table 2: Orbital elements

Element	Name	Units
$\alpha$	semi-major axis	AU
$e$	eccentricity	-
$i$	Inclination	deg
$\Omega$	Longitude of the ascending node	deg
$\omega$	Argument of the perihelion	deg
M	Mean anomaly	deg

- $\alpha$

The semi-major axis of the elliptical asteroid orbits in AU. For main belt asteroids  $2 < \alpha < 3.3$  AU approximately.

- $e$

The eccentricity of the orbit ( $e = c/a$  where  $c$  is the distance between a focus and the center of the ellipse) with values  $0 < e < 1$ . Most main belt asteroids have  $e < 0.3$ .

- $i$  (Inclination)

The angle between the plane of an asteroid orbit and the ecliptic. Most asteroids have  $i < 25^\circ$ .

- $\Omega$

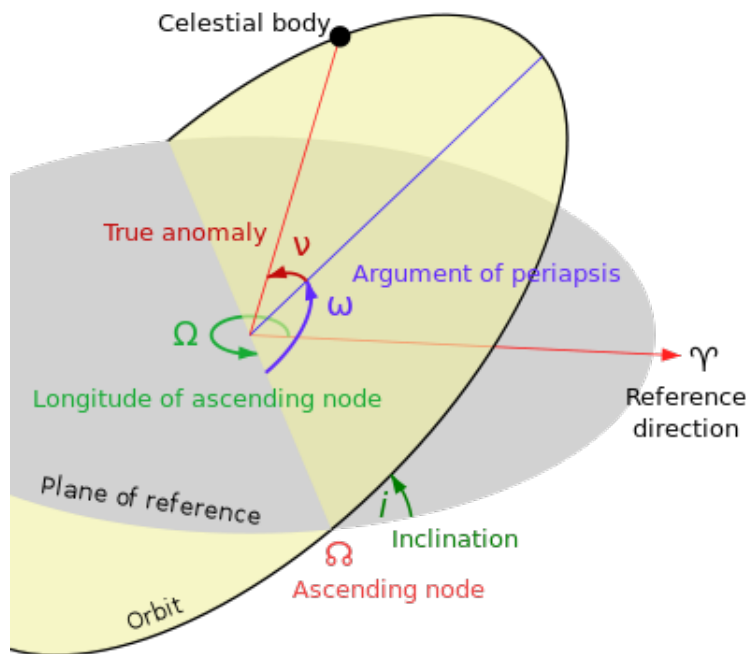
The direction of the line where the orbital plane intersects the plane of the ecliptic. It is measured from the vernal equinox point ( $\gamma$ ).

- $\omega$

The angle between the ascending node and the perihelion point measured in the direction of motion. It defines how the major axis of the orbit is oriented in the orbital plane.

- M (Mean anomaly)  
 Defines the position of the orbiting body along the ellipse at a specific time.

Figure 3: The orbit plane of a celestial object (in this case of an asteroid) with respect to a plane of reference (in this case to the ecliptic) and the orbital elements.



All asteroids are subjected to gravitational forces from the planets and the rest of the asteroids. These perturbations cause changes to the asteroid orbits over time. The orbital elements are known as osculating elements and change in a quasi-periodic and predictable manner. In the Solar System, such changes usually occur on timescales of thousands of years. Instead of the osculating, the *proper elements* are more commonly used. They refer to a set of orbital elements calculated by ignoring perturbations and can be described as representing the average motion of the body concerned. For most bodies, the osculating elements are relatively close to the proper elements because precession and perturbation effects are relatively small.

Besides the orbital elements of the asteroids' orbits, there are other values that can define some of their characteristics, such as the albedo, absolute magnitude and slope parameter.

#### **Albedo**

Albedo is the fraction of light that is reflected by a body or surface. Its value ranges from 0, for a perfectly black surface, to 1, for a totally reflective surface.

#### **Opposition Effect**

As an asteroid approaches opposition it will usually brighten 0.3–0.5 magnitudes. It varies with asteroid type and albedo. Low albedo values indicate small opposition effect.

#### **Absolute magnitude (H)**

The absolute magnitude of an asteroid is the Visual magnitude an observer would record if the asteroid were placed 1 Astronomical Unit (AU) away (from the Earth), 1 AU from the Sun and at a zero phase angle (fully illuminated). It is geometrically impossible, but H is very useful because it can be converted to diameter. The lower the H value, the larger the size of the object. This conversion requires the knowledge of the asteroid's albedo, but the albedo for most asteroids is not known. An albedo range between 0.25 to 0.05 is usually assumed.

#### **Slope parameter (G)**

When the object is near opposition, an increase in brightness is observed, typically 0.3 magnitudes. Its value depends on the way light is scattered by particles on the asteroid's surface. It is known only for a small number of asteroids. For most asteroids a value of 0.15 is assumed.

## **1.5 Composition of asteroids**

The asteroids can be classified by their composition which depends on their distance from the Sun. This means that they lie at approximately the distance where they originally formed. By using telescopes to measure the colour, reflectivity and the spectra of asteroids and the use of radars, astronomers can determine the composition of asteroids and their mineral properties. An asteroid classification system was first devised in 1975 by Chapman, Morrison, and Zellner. It included just three classes: (C) dark carbonaceous objects which make up 75% of known asteroids, (S) stony or siliceous objects, 17% of known asteroids and (U) for all others. The original system has been expanded by Tholen and, more recently, the SMASS

(Small Main-Belt Asteroid Spectroscopic Survey) classification. The former included 14 types that the latter expanded to 24. The SMASS classification was introduced by Schelte J. Bus and Richard P. Binzel in 2002 and was based on data collected from 1447 asteroids. These are called *spectral types* because they were based on the asteroids' different spectra. Their spectra are similar to the Sun's but with differences due to various minerals on the surface of the asteroid reflecting sunlight differently.

Between 2.7 AU and 3.5 AU over 80 % of the asteroids are C-type. These asteroids contain large quantities of carbon molecules and are almost coal-black reflecting only about 4% of the light that strikes them. They are very similar in composition to the carbonaceous chondrite meteorites that sometimes fall on Earth. At 2 AU, only 40% of asteroids are C-type. At this distance most asteroids are grey and made of silicate compound rock. Some of the asteroids closest to the Sun receive enough radiation to melt, differentiate and develop iron cores.

Asteroids less than 100–150 m in diameter are solid bodies (monoliths) most likely fragments of larger asteroids broken up by collisions. Objects larger than this and under 300 m in diameter are loose collections of fragments held together by the force of their gravity, usually described as *rubble piles*. These asteroids were formed in collisions. If their rotation period becomes less than 2-2.5 hours, they will disintegrate.

The shapes of the larger asteroids, with a diameter of more than few hundred kilometers, are more “round” and, most likely, differentiated, consisting of layers of material. The spherical shape is a result of gravitational forces, and the differentiation is due to heating, by the decay of radioactive elements, during formation.

## 1.6 Main belt asteroid Families

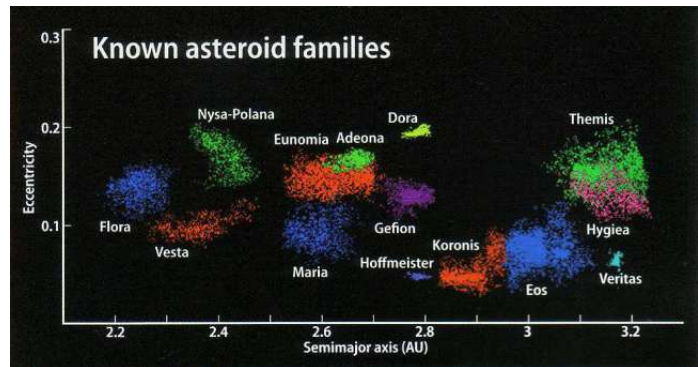
Groups of asteroids within the main belt which share similar mean orbital elements (semimajor axis, eccentricity, and inclination) are called families. Asteroid families are formed when an asteroid is disrupted in a catastrophic collision, the members of the family thus being pieces of the original asteroid. The members of a family usually have matching compositions. Exceptions are the families which were formed from a large differentiated parent body (such as the Vesta family). Most asteroid families are found in the main asteroid belt, although several family-like groups lie at smaller semi-major axis distances or larger inclination than the main belt. Asteroid families

are thought to have lifetimes of the order of a billion years. The age of the Solar system is about 4.6 billion years which means that the families observed now have not been the same since the formation of the solar system. Decay of families occurs because of both slow dissipation of the orbits due to perturbations from Jupiter or other large bodies, and because of collisions between asteroids which grind them down to small bodies.

Table 3: Prominent Main asteroid belt families

Family name	$\alpha(AU)$
Eos	2.99 to 3.03
Eunomia	2.53 to 2.72
Flora	2.15 to 2.35
Hygiea	3.06 to 3.24
Koronis	2.83 to 2.91
Maria	2.5 to 2.71
Nysa	2.41 to 2.5
Themis	3.08 to 3.24
Vesta	2.26 to 2.48

Figure 4: Asteroid families



## 1.7 Binaries

A binary asteroid is a system of two asteroids orbiting their common center of mass. When the two asteroids orbiting around each other are similarly sized are called binary companions or double asteroids. Many asteroids possess one or more small moons. Such binaries are formed when small, irregularly shaped ‘rubble pile’ asteroids have their rotation rates increased by the YORP effect which is a result of the absorption and subsequent re-emission of solar radiation. If the rotation period becomes less than 2–3 h, material will be shed which may accumulate to form one or more small, nearby satellites. 243 Ida was the first asteroid to be found, in 1994 on images taken by the Galileo spacecraft, to have a natural satellite, Dactyl. In the Main belt there are also triple asteroids, 45 Eugenia and 87 Sylvia being the first to be discovered.

Figure 5: 243 Ida and its moon Dactyl.



## 1.8 Yarkovsky and YORP effects

The Yarkovsky effect is caused by sunlight and describes a small but significant force that affects the orbital motion of small bodies. Its influence is most significant to meteoroids or small asteroids (diameter  $< 30 - 40\text{Km}$ ). The effect was discovered by the Russian civil engineer Ivan Osipovich Yarkovsky

(1844–1902). Around the year 1900, Yarkovsky noted that the diurnal heating of a rotating object in space would cause it to experience a force that could lead to large long-term effects on the orbits of small bodies. These bodies absorb radiation from the Sun, but there is a delay in emission of this energy as heat. The warmest point on a rotating body occurs after noon, thus there is a difference between the directions of absorption and emission of radiation which creates a small thrust. For a prograde asteroid, the force is in the direction of motion of the orbit, so its orbit will gradually expand, while the orbit of a retrograde asteroid will shrink. This is called the *diurnal effect* and is the dominant component for asteroids greater than 100 m diameter. The effect was first measured in 1991–2003 on the asteroid 6489 Golevka. The asteroid drifted 15 km from its predicted position over twelve years.

The Yarkovsky–O’Keefe–Radzievskii–Paddack effect (YORP effect) is another variation on the Yarkovsky effect and changes the rotation of asteroids (and of small bodies in general). When a rotating body emits infrared radiation (because it has been heated by the Sun), each photon carries away momentum. YORP can spin up asteroids so fast that if they are rubble piles, they will disintegrate or “shed mass,” which is one way of creating asteroid satellites. A direct observational confirmation of the YORP effect happened in 2007 through precise measurement of changes in the spin rates of the asteroids 54509 YORP (Lowry et al. and Taylor et al.) and 1862 Apollo (Kaasalainen et al.).

## 2 Studying Asteroids

Some ways to collect data and get information about asteroids are space missions and orbiting observatories, spectroscopy, study of meteorites, radar observations and photometric observations.

### 2.1 Space missions

Some of the current and past missions that give information about asteroids are:

- *Dawn*  
It studied (4) Vesta from July 2011 to September 2012 and now is on its way to the dwarf planet (1) Ceres (NASA).
- *The Japanese Aerospace Exploration Agency's Hayabusa spacecraft*  
In 2010, it has brought to Earth tiny pieces of the asteroid Itokawa (1998 SF36).
- *New Horizons*  
It has been scheduled to arrive at dwarf planet (134340) Pluto in 2015 (NASA).
- *The Near-Earth Object Surveillance Satellite (NEOSSat)*  
It is a Canadian satellite and launched on February 25<sup>th</sup>, 2013. It is the first space telescope dedicated to detecting and tracking asteroids and satellites.
- *Don Quixote*  
It will test a method of deflecting an Earth-approaching asteroid (ESA).
- *The Origins Spectral Interpretation Resource Identification Security - Regolith Explorer spacecraft (OSIRIS-REx)*  
It will travel to a near-Earth asteroid, called Bennu (formerly 1999 RQ36), and bring at least a sample back to Earth for study. The mission will help scientists investigate how planets formed and how life began, as well as improve our understanding of asteroids that could impact Earth. OSIRIS-REx is scheduled for launch in late 2016. The

spacecraft will reach its asteroid target in 2018 and return a sample to Earth in 2023 (NASA).

- *The Mercury Surface Space Environment Geochemistry and Ranging mission* (MESSENGER)

It will look for the elusive Vulcanoids as a secondary objective to its primary target of the planet Mercury (NASA).

- *The Near-Earth Asteroid Rendezvous spacecraft* (NEAR)

It completed its trip to asteroid (433) Eros with a soft landing on that asteroid in 2001 (NASA).

- *Galileo*

On its way to Jupiter flew past main belt asteroid 951 Gaspra on 29 October 1991 and obtained the first high resolution images of an asteroid. On 28 August 1993, the spacecraft had a close encounter with main belt asteroid 243 Ida (NASA).

- *Cassini*

On its way to Saturn, crossed the Asteroid Belt and took pictures of asteroid 2685 Masursky on 23 January 2000. The images revealed that the side of Masursky imaged by Cassini is roughly 15 - 20 km across (NASA/ESA).

- *Rosetta*

During its 10 year journey towards comet 67P/Churyumov-Gerasimenko, the spacecraft has passed by two asteroids: 2867 Steins (in 2008) and 21 Lutetia (in 2010). The spacecraft entered deep-space hibernation mode in June 2011, and “woke up” on 20 January 2014. Rosetta will arrive at the comet in August 2014 (ESA).

Additionally Earth-orbiting observatories have targeted or will observe asteroids, such as:

- The Wide-field Infrared Survey Explorer (WISE) mission (NASA).
- The InfraRed Astronomy Satellite (IRAS)
- Gaia mission (ESA)

## 2.2 Spectroscopy

A way to study asteroids is through spectroscopy. By analyzing an asteroid's spectrum, the kind of materials on its surface can be deduced. The sunlight reflects off of an asteroid but the asteroid spectrum differs from the spectrum we get from the Sun. This is because the sunlight is transmitted to some depth within the material before being reflected. Because different materials absorb different parts of the spectrum, the fraction of light that is reflected to Earth can vary as a function of wavelength, depending on the optical properties of the mineral grains. By determining which wavelengths of the spectrum were absorbed, we can discover the materials of an asteroid's surface.

Most of the asteroids that have been analyzed are large main belt asteroids. From the data collected we can realise that there is a correlation between asteroids and meteorites, though harder asteroids would survive more frequently while they enter Earth's atmosphere and thus be better represented in meteorites. Spectroscopy gives an average composition of the surface. We cannot see detailed variations over the surface, except hemispheric variations as the asteroid rotates.

The surface composition of asteroids varies with respect to their distance from the Sun. The distant ones have water and carbonaceous chondrites on their observable surfaces. Asteroids that are closest to the Sun are more stony-iron on the surface and stay considerably cooler underneath the surface and thus probably have higher concentrations of volatiles under it.

## 2.3 The study of meteorites

Meteorites are non-terrestrial rocks found on the surface of the Earth and have many different origins such as asteroids, comets, Mars, even the Moon. The vast majority of meteorites come from asteroids, and they are the most ancient rocks studied. They are pieces of larger bodies that were broken apart or had fragments chipped off during collisions and some of these fragments were thrown into orbits that eventually intersected Earth's. Not all the pieces of space debris that enter Earth's atmosphere reach our planet's surface. Only larger asteroids and asteroid fragments can survive. The majority burn up in the atmosphere and are called "shooting stars".

By comparing their reflectance spectra, different groups of meteorites can be connected with classes of asteroids. For example, stony meteorites corre-

spond to stony asteroids (outer rocky layers, or undifferentiated asteroids), iron meteorites to metal-rich asteroids (fragments of dense cores inside differentiated bodies), and carbonaceous meteorites to the dark C-type asteroids (black, carbonaceous asteroids).

Most meteorites fall into one of four categories. The first three categories apparently have their origins in parent bodies that were gravitationally differentiated, as opposed to the fourth category.

- *Iron meteorites*

They are usually one piece of iron-nickel (Fe-Ni) metal. The ratio of nickel ranges from 5% to 62% with an average of 10% nickel. Most iron meteorites are nearly pure metal, but there are some metal meteorites with up to 30% mineral inclusions such as sulfides, metal oxides and silicates. The iron meteorites (4%) show that some asteroids differentiated completely forming iron cores.

- *Stony irons*

They consist of mixtures of Fe-Ni metal of between 30% and 70% along with mixtures of various silicates and other minerals. The Fe-Ni metal can be present as chunks, pebbles and granules. Stony irons probably were parts of the outer cores or mantles.

- *Achondrites*

They are silicate rich meteorites apparently formed by molten or volcanic activity in their parent bodies, and consist of a broad range of minerals. Achondrites are the result of gravitational differentiation in relatively large bodies and most resemble the Earth's crust.

- *Chondrites*

Most of meteorites are from stony bodies that never differentiated. They probably came from parent bodies that were too small to undergo gravitational differentiation, or are collision ejecta from collisions of slightly differentiated bodies. Most stony meteorites, and all carbonaceous meteorites, are chondrites. These rocks are primeval fragments of the solar system's original mineral grains. Dating by the technique of radioactive decay shows that the most primitive meteorites formed during an interval of only 20 million years, some 4.6 billion years ago.

## 2.4 Radar observations

Some other techniques which can also reveal information on the asteroid's size, surface features, shape and subsurface consistency include the use of radar, radio wave observations, interferometry and stellar occultation. The two main radars used for planetary radar astronomy are the National Astronomy and Ionosphere Center's Arecibo Observatory in Puerto Rico and NASA's Goldstone Solar System Radar in California. Arecibo has twice the range and can see three times the volume of Goldstone, while Goldstone, whose greater steerability provides twice the sky coverage and much longer tracking times, serves a complementary role. Additional radars used occasionally to analyze near Earth asteroids are in Japan, Russian and Germany.

Asteroid Radar Astronomy started with the detection of near-Earth asteroid (1566) Icarus on June of 1968 at Haystack and at Goldstone. The first asteroid detection at Arecibo was that of (433) Eros in 1975, which was also detected at Goldstone. The first detection of a main belt asteroid, (1) Ceres, took place at Arecibo in 1977. The detection rate of asteroids was  $<10$ /year until the upgrade of the Arecibo radar in the late 1990s. Since then, dozens of asteroids have been detected each year.

## 2.5 Photometric observations

### 2.5.1 Asteroid rotation

The rotational angular momentum ( $\bar{L}$ ) of an asteroid is

$$\bar{L} = \hat{I}\bar{\omega} \quad (1)$$

where  $\bar{\omega}$  angular velocity and  $\hat{I}$  the inertia tensor.

The angular momentum vector and the inertia tensor are changed through processes of asteroid evolution such as collisions. The inertia tensor is a symmetric tensor with six independent components, but a system of coordinates in the asteroid-fixed frame that gives zero non-diagonal components can also be chosen (so that the inertia tensor has only 3 components). The diagonal components  $I_x \leq I_y \leq I_z$  are then the principal moments of inertia. The axes are called the principal inertia axes.

Asteroids that do not rotate about one of their principal axis (Non-Principal Axis – NPA) are referred to as tumblers. This spin can be seen as a composition of two (or more) rotational periods. Tumbling motion is a

non-efficient rotation that put the asteroid in a high or excited energy state. The asteroid is not a completely rigid body so the excess rotational energy is dissipated in the asteroid's interior and the spin state asymptotically reaches the lowest energy state, which is a rotation around the principal axis of the maximum moment of inertia  $I_z$ . An approximation for the timescale of the damping ( $\tau$ ) of the excited rotation to the lowest energy state of principal-axis rotation has been derived by Harris (1994):

$$\tau = \frac{P^3}{C^3 D^2} \quad (2)$$

where  $P$  is the rotation period ( $P = 2\pi/\omega$ ) in hours,  $D$  is the mean diameter of the asteroid in Kilometers, and  $C$  is a constant of about  $17 \pm 2.5$ , for  $\tau$  in billions ( $10^9$ ) of years. Most of the asteroids have damping time scales shorter than their presumed age but small and slow rotating asteroids might show tumbling motion. Observations show that tumbler asteroids rotate slowly. Tumbling does not make an asteroid rotate slowly, but rather slow rotating asteroids manage to keep their tumbling motion. Tumbling rotation can be caused by collisions, tidal forces following an encounter with a planet, radiation forces such as YORP, or mass ejection.

The asteroid's angular momentum vector cannot be measured with observations. The observable parameter is the spin vector. The angular momentum can be estimated using equation (1) with an estimate of the moment of inertia based on the asteroid shape, size, and bulk density. The most frequently used method of derivation of the spin vector from ground based observations, is lightcurve observations. Lightcurve observations require a lot of observing time (many nights over several years) to gather enough data for a full solution of the spin vector. However, an estimate of the rotation period can be obtained from observations of only a few nights.

The rotation periods and pole directions of asteroids can be affected by collisions and the thermal radiation force (YORP effect). The rotational states of the asteroids combined with their shapes and orbits, reflect their collisional history. How we see the rotation of an asteroid depends on its position and the orientation of its spin axis with respect to Earth and the Sun. The rotation period of an asteroid is typically several hours.

### 2.5.2 Size dependence of the rotation rates

The spin rate distribution of large asteroids ( $D > 40\text{km}$ ) fits a Maxwellian distribution. A lower bound diameter for the large asteroid group has been estimated between 30 and 50 Kilometers. The range between 10 and 40 Km is considered a transitional region where the small and large asteroid groups overlap. Pravec and Harris (2000) give a lower limit of 40km.

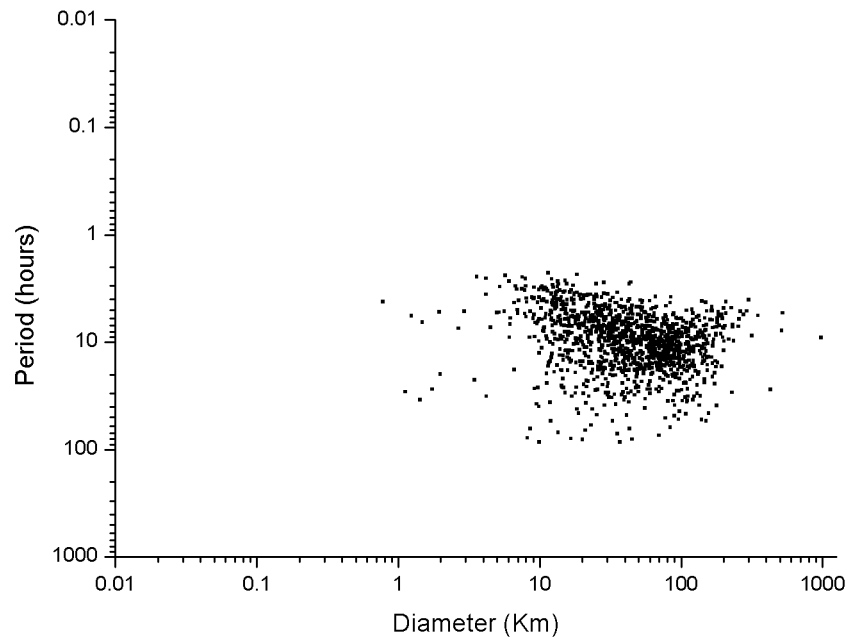
The Maxwellian distribution has the form (P.Pravec, A.W.Harris, T.Michalowski *Asteroid Rotations*):

$$n(f) = \sqrt{\frac{2}{\pi}} \frac{N f^2}{\sigma^3} \exp\left(\frac{-f^2}{2\sigma^2}\right)$$

where  $f$  is spin rate (revolutions per day),  $n(f)df$  is the fraction of objects in the range  $(f, f+df)$ ,  $N$  is the total number of objects and  $\sigma$  is the dispersion.

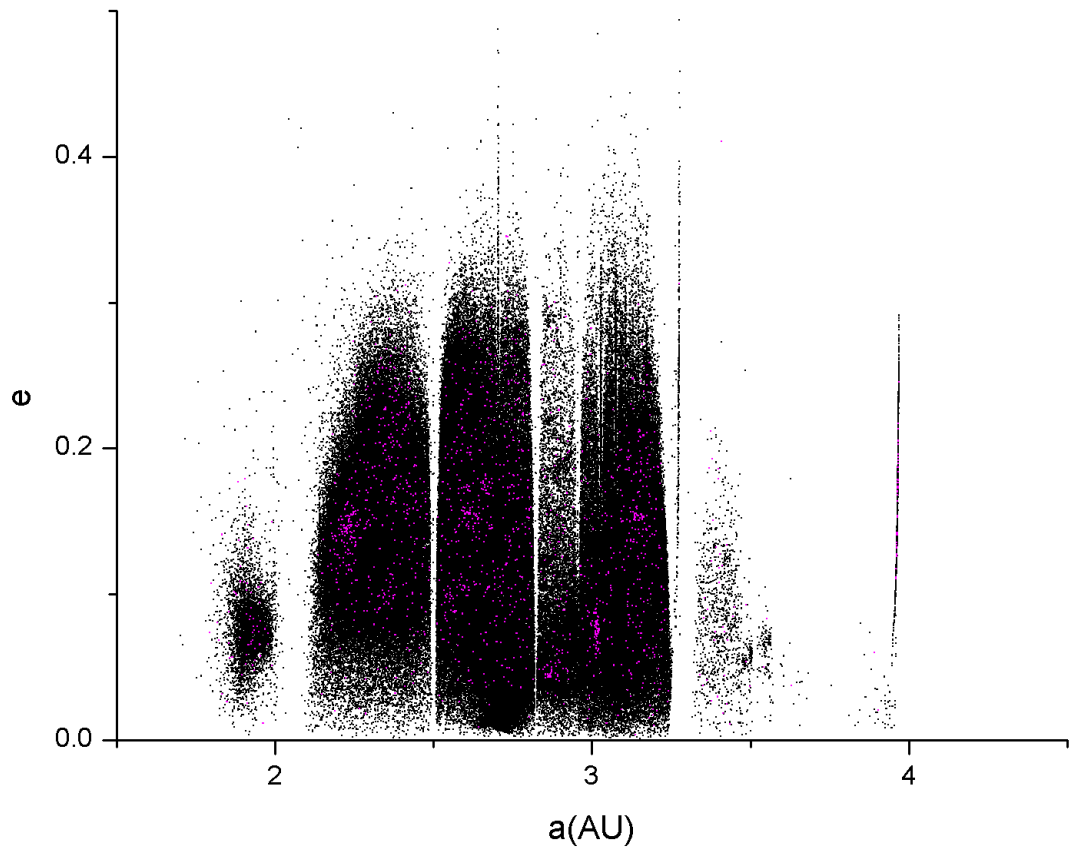
In Fig. 6 the rotation period vs diameter is plotted using data of 1279 asteroids.

Figure 6: A diagram of period vs diameter. The rotation periods can be found on the URL: <http://www.minorplanetcenter.net/iau/lists/LightcurveDat.html> and the diameters on <http://vizier.u-strasbg.fr/viz-bin/VizieR-4>



The asteroids whose periods were used for the period-diameter diagram are shown in Fig. 7 . The sample taken is from asteroids with known period in 2006 (1279). Now (2014), the asteroids with known period are over 4000.

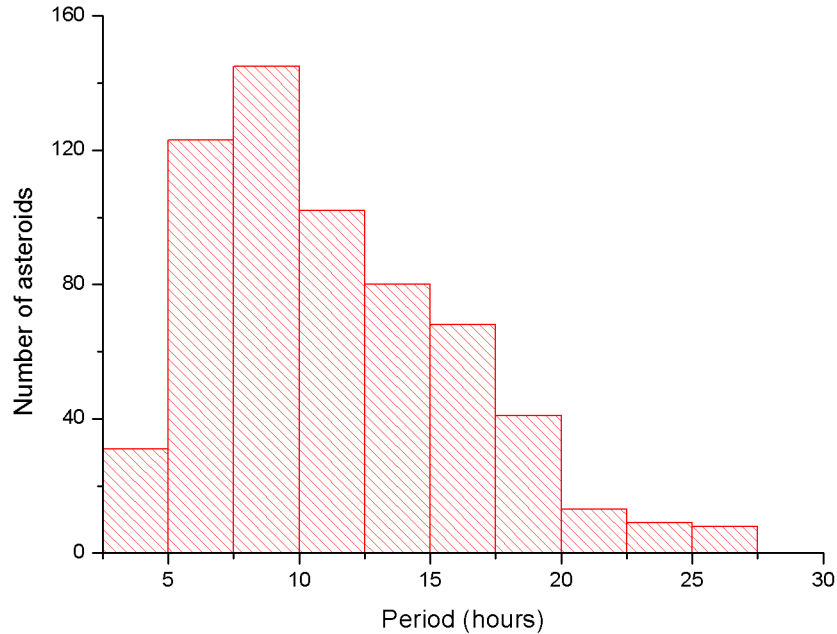
Figure 7: An a-e diagram in which we can see the asteroids with known period



Deviations from the Maxwellian distribution of rotation rates are expected because the sample of asteroids is not homogenous. Asteroids have different masses and properties.

However, in order to conclude that the spin rate distribution is Maxwellian for larger asteroids but non-Maxwellian below a certain diameter, an assumption of a constant dispersion for asteroids of all sizes has been made in each sample, which is an incorrect assumption.

Figure 8: An histogram for asteroids with diameter  $D > 40\text{Km}$ . A sample of 668 asteroids has been used. Slow rotators ( $P > 27\text{h}$ ) have been excluded.



### 2.5.3 Asteroid rotation period and Lightcurves

Photometry is the measurement of the brightness of a celestial object. The magnitude of an asteroid is calculated by comparing its brightness with that of a comparison star or stars of known magnitude. A lightcurve is a plot showing variation in magnitude with respect to time. The two primary parameters of a lightcurve are the period and the amplitude. Asteroids have irregular shapes, thus when they rotate, they will reflect different amounts of light as time goes on. As an asteroid rotates, we see different areas presented and so the reflected light varies in intensity. When a lightcurve starts repeating it means that the asteroid completed a rotation. The rotation period is calculated from the length of the lightcurve. The most common shape of lightcurves is sinusoidal with two maximum and two minimum, with different

height and depth. Additionally, the lightcurve amplitude gives us information about the asteroid shape. For example potato-shaped or cigar-shaped asteroids have large amplitude values. The amplitude of the lightcurve may not be the same at each opposition. Any asteroid might be seen broadside to its axis of rotation at one opposition and along the axis of rotation at another.

Like for all the astrophysics areas, with the introduction of Charge Coupled Devices (CCDs), there has been a considerable progress in asteroid photometry.

Besides the period of rotation, the lightcurve of an asteroid can be used to determine its shape:

- By obtaining lightcurves at a given apparition and repeating the process at several apparitions we can determine the orientation of the rotation axis and eventually a model for its shape.
- Shape determinations can be assisted by observations during an occultation, when the asteroid passes in front of a star.
- Observations taken at the same time as radar observations can allow a better determination of an asteroid's size and shape.

In addition, asteroid lightcurves give us information about their composition (solid bodies or rubble piles), their size (in conjunction with observations in the infrared), their correlation between period and size, spectral class or location in the main belt. Finally, long term photometric observations of a given asteroid helps to determine the absolute magnitude and the slope parameter which define the brightness of the asteroid.

### **Shape and Spin Axis Modeling**

An asteroid can be described as a triaxial (or scalene) ellipsoid. The best results for shape and spin axis modeling come when lightcurves are obtained over a large range of phase angles within an apparition. A method called *The lightcurve inversion method* has been developed (Kaasalainen et al. 2001, Kaasalainen & Torppa 2001) for the determination of the direction of the spin axis.

### 3 Observations and instrumentation

#### 3.1 Holomon Astronomical Station

Holomon Astronomical Station (HAS) was an initiative of Prof. John Seiradakis (Observatory of Thessaloniki, Department of Physics). It is located inside the Aristotle University’s Forestry Department’s Campus at Mt. Holomon Chalkidiki and was a kind offer from the Aristotle University’s Forest Director, Mr. G.Panourgias. The geographical coordinates of Holomon Astronomical Station are:

$$\lambda = 23\ 30\ 19.6\ E$$

and

$$\phi = 40\ 25\ 58.4\ N$$

its altitude is 900 m.

#### 3.2 Observation dates and equipment used

The instruments that were used for the observations were: two Schmidt-Cassegrain telescopes with diameters 10in and 11in (25.4cm and 27.9cm respectively), two CCD cameras (ATIK 11000, FingerLakesPL6303E) and two german equatorial mounts. The mounts and CCD cameras were controled with MaxIm DL software and the pictures were processed with MPO Canopus. The procedure that followed was differential photometry which means that the difference between a target and comparison (or average of several comparisons) using instrumental magnitudes is found for each image. The images were reduced using bias and dark subtraction and division by a flat-field image.

Table 4: Telescopes used

	Diameter(cm)	Focal Length (mm)	Focal Ratio
1	25.4	2500	f/10
2	27.9	2800	f/10

The dates of observations (YYMMDD) for each asteroid and also the equipment that was used are shown at the following table:

Table 5: CCD cameras used

	Pixels	Pixel size ( $\mu \times \mu$ )	Quantum efficiency	Readout Noise
ATIK 11000	4008x2672	9x9	50%	$13e^-$
FLI	3072x2048	9x9	68%	$9e^-$

Table 6: Targets and observations dates

Asteroid	Observation date	Telescope used	CCD camera used
354 Eleonora	20120805	10in	ATIK11000
354 Eleonora	20120807	10in	ATIK11000
79 Eurynome	20121001	10in	ATIK11000
213 Lilaea	20130428	10in	ATIK11000
213 Lilaea	20130429	10in	ATIK11000
213 Lilaea	20130502	10in	ATIK11000
173 Ino	20130502	11in	FLI
173 Ino	20130504	11in	FLI
173 Ino	20130725	10in	ATIK11000
173 Ino	20130726	10in	ATIK11000
173 Ino	20130727	10in	ATIK11000
173 Ino	20130728	10in	ATIK11000
374 Burgundia	20130808	10in	ATIK11000
374 Burgundia	20130809	10in	ATIK11000
374 Burgundia	20130810	10in	ATIK11000

### 3.3 Target selection

The aim of this diploma thesis was the determination of rotation periods of asteroids from the main belt. Hence no filters were used. Also for good signal-to-noise ratio without the need for the exposure time to increase dramatically, the asteroids chosen are no fainter than magnitude 13. The SNR defines the ratio between the signal from the target with respect to the total signal received. An adequate value for SNR is 100 (noise is 1% of the total signal) which means that the precision will be 0.01mag. However, if the observed asteroid has an amplitude larger than 0.2mag, good results can be obtained even with a SNR near 50. This can be converted to an error in magnitudes by  $1.0857 / \text{SNR}$ . Observations with  $\text{SNR} < 10$  will have very low precision

(> 0.1mag) and should not be used.

Another factor that had to be taken into consideration was the altitude of the asteroid because of the morphology of the location. With buildings and trees blocking parts of the sky, asteroids with declination greater than  $-15^\circ$  were chosen.

The data for the asteroid selection were acquired from the following URL:

[http://www.minorplanet.info/PHP/call\\_OppLCDBQuery.php](http://www.minorplanet.info/PHP/call_OppLCDBQuery.php)

and the Ephemeris data were obtained from:

<http://www.minorplanetcenter.net/iau/MPEph/MPEph.html>.

Five asteroids were selected: 354 Eleonora, 79 Eurynome, 213 Lilaea, 374 Burgundia and 173 Ino.

The diameter of the five asteroids and their location in the main belt versus their eccentricity and inclination are shown in the following table and in the two diagrams.

Table 7: Diameters in Km of the five targets

Asteroid	Diameter (Km)
374 Burgundia	44.67
79 Eurynome	66.47
213 Lilaea	83.01
173 Ino	154.10
354 Eleonora	155.17

Figure 9: The five observed asteroids in an a-e diagram

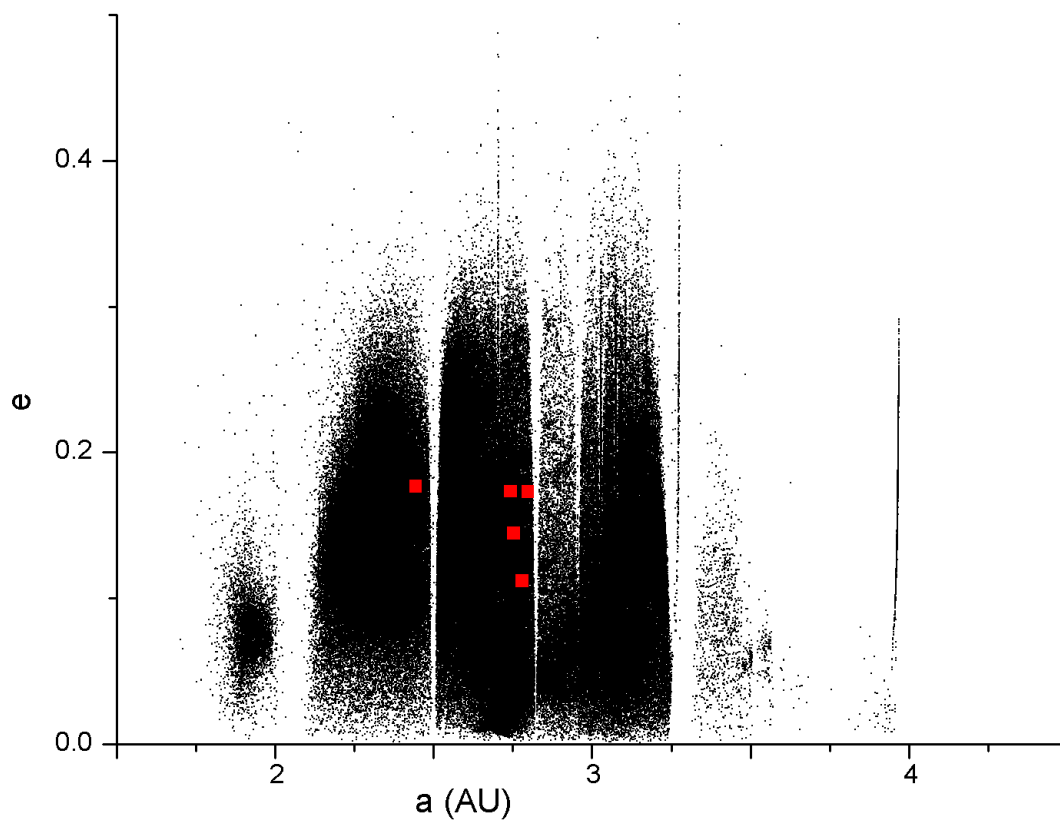
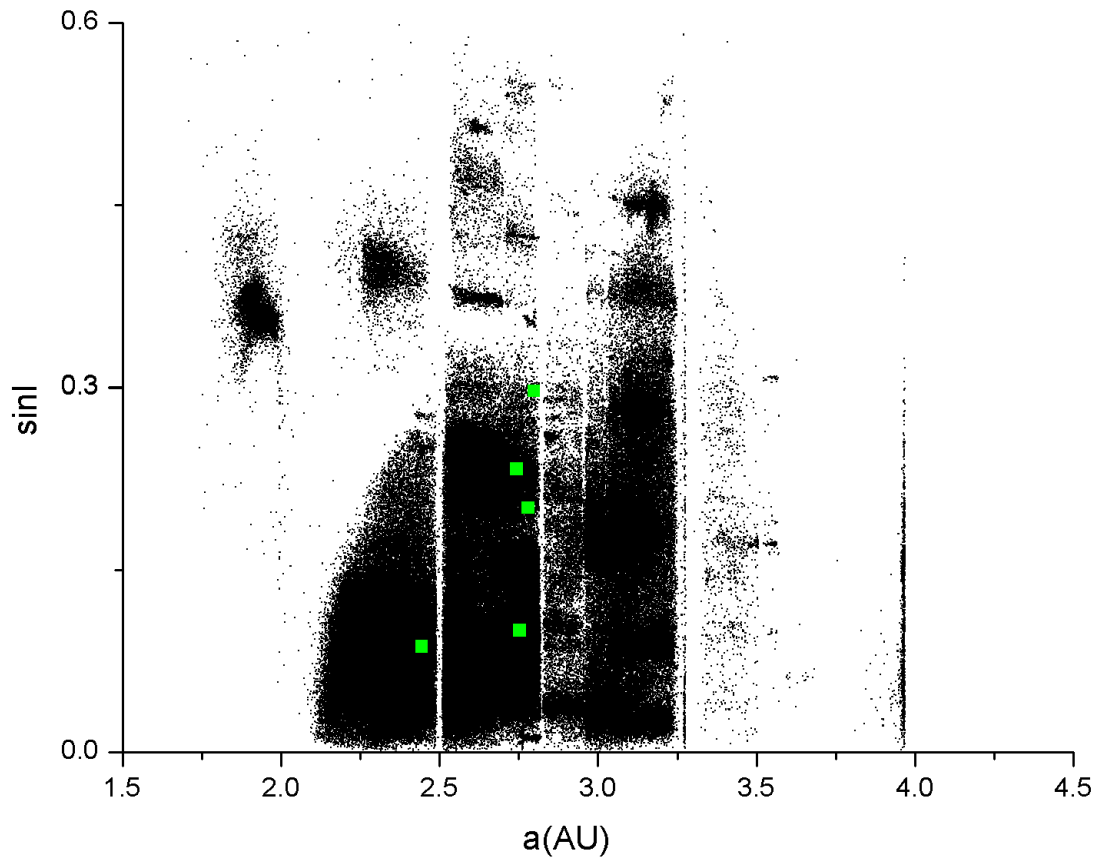


Figure 10: The five observed asteroids in an a-sinI diagram



Data from Ephemeris for the five asteroids that have been observed are shown in the following table. Ephemeris for each date is for 20:00 UT. Dates are written in the form YYMMDD, RA and Dec correspond to the right ascension and declination of the object, Mag is the visual magnitude, Ph is the asteroid's phase (angle between Sun-asteroid-Earth),  $r$  is the distance from the Sun in Astronomical Units and SM is the Sky Motion of asteroids in  $''/\text{min}$ .

Table 8: Ephemeris for the observed asteroids

Asteroid	Date	RA	Dec	Mag	Ph	r	SM
354 Eleonora	20120805	22 05 02.2	-13 30 36	10.9	4.8	3.119	0.57
354 Eleonora	20120807	22 03 38.2	-13 48 29	10.8	4.1	3.119	0.58
79 Eurynome	20121001	23 59 09.3	+03 31 03	10.0	4.0	2.065	0.62
213 Lilaea	20130428	13 57 51.1	-00 16 10	12.2	6.0	2.583	0.56
213 Lilaea	20130429	13 57 01.9	-00 12 17	12.2	6.3	2.582	0.55
213 Lilaea	20130502	13 54 36.6	-00 01 33	12.3	7.4	2.577	0.53
173 Ino	20130502	19 40 31.0	-07 22 21	12.9	20.6	2.749	0.35
173 Ino	20130504	19 41 29.1	-07 14 46	12.8	20.5	2.745	0.33
173 Ino	20130725	19 09 51.3	-09 05 27	11.4	7.8	2.566	0.61
173 Ino	20130726	19 09 03.0	-09 13 02	11.4	8.1	2.564	0.60
173 Ino	20130727	19 08 15.5	-09 20 42	11.4	8.4	2.562	0.60
173 Ino	20130728	19 07 28.8	-09 28 27	11.4	8.8	2.560	0.59
374 Burgundia	20130808	21 02 51.8	-02 01 12	12.4	5.3	2.693	0.55
374 Burgundia	20130809	21 02 03.3	-02 05 34	12.4	5.3	2.694	0.55
374 Burgundia	20130810	21 01 14.9	-02 10 04	12.4	5.3	2.695	0.55

## 4 Results for asteroids 354 Eleonora, 79 Eurynome, 213 Lilaea, 374 Burgundia and 173 Ino

The results of the observations are presented below. First the raw data from every night are shown and then the composite lightcurve for each asteroid is constructed.

### 4.1 354 Eleonora

354 Eleonora is a large, main-belt asteroid that was discovered by the French astronomer Auguste Charlois on January 17, 1893. Eleonora was classified by Zellner and Bowell (1977) as an S type object. The first photoelectric observations of Eleonora were performed by Groeneveld and Kuiper (1954) on two consecutive nights. They found a period of rotation  $P_{syn} = 4^h.27$ . Chang and Chand (1963) after observing 354 for three nights confirmed the previous period, with a maximum amplitude of 0.30mag. Zappala *et al.*

published their lightcurves (1978) with  $P = 4.2772 \pm 0.0002h$  and Kevin Ivarsen, Sarah Willis, Laura Ingleby, Dan Matthews, Melanie Simet (CCD observations and period determination of fifteen minor planets, Volume 31, Number 2, A.D. 2004 April-June, The Minor Planet Bulletin, Bulletin of the Minor Planets Section of the association of lunar and planetary observers) published their lightcurves again with a period  $P = 4.2772 \pm 0.0001h$  and amplitude  $amp = 0.15$ . At the following table and figures are shown its orbital elements at Epoch 2456800.5 (2014-May-23.0) (Reference: JPL 79) heliocentric ecliptic J2000 and the lightcurve resulting from the Holomon Astronomical Station data with period  $P = 4.277 \pm 0.002h$  and approximate amplitude  $amp = 0.15mag$ .

Table 9: Orbital elements of 354 Eleonora

Element	Value
a	2.79868 AU
e	0.115352
i	18.398 deg
$\Omega$ (node)	140.378 deg
$\omega$ (peri)	5.944 deg
M	314.932 deg
Absolute Magnitude (H)	6.4 mag
Slope parameter (G)	0.37 mag
Perihelion (q)	2.4758 AU
Aphelion (Q)	3.1215 AU
Orbital period	1710.12 days
Diameter	155.17 km
Geometric albedo	0.1948
Rotation period	4.277h

The ecliptic longitude of the spin axis direction (J2000.0, in degrees) ( $\lambda$ ) and the ecliptic latitude of the spin axis direction (J2000.0, in degrees) ( $\beta$ ), were calculated with the lightcurve inversion method:

$$\lambda = 144^\circ$$

and

$$\beta = 54^\circ$$

Figure 11: Shape model of 354 Eleonora (DAMIT = Database of Asteroid Models from Inversion Techniques)

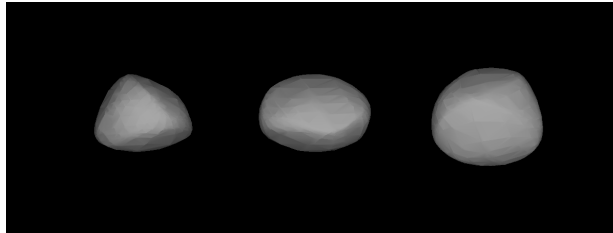


Figure 12: Raw data 2012/08/05

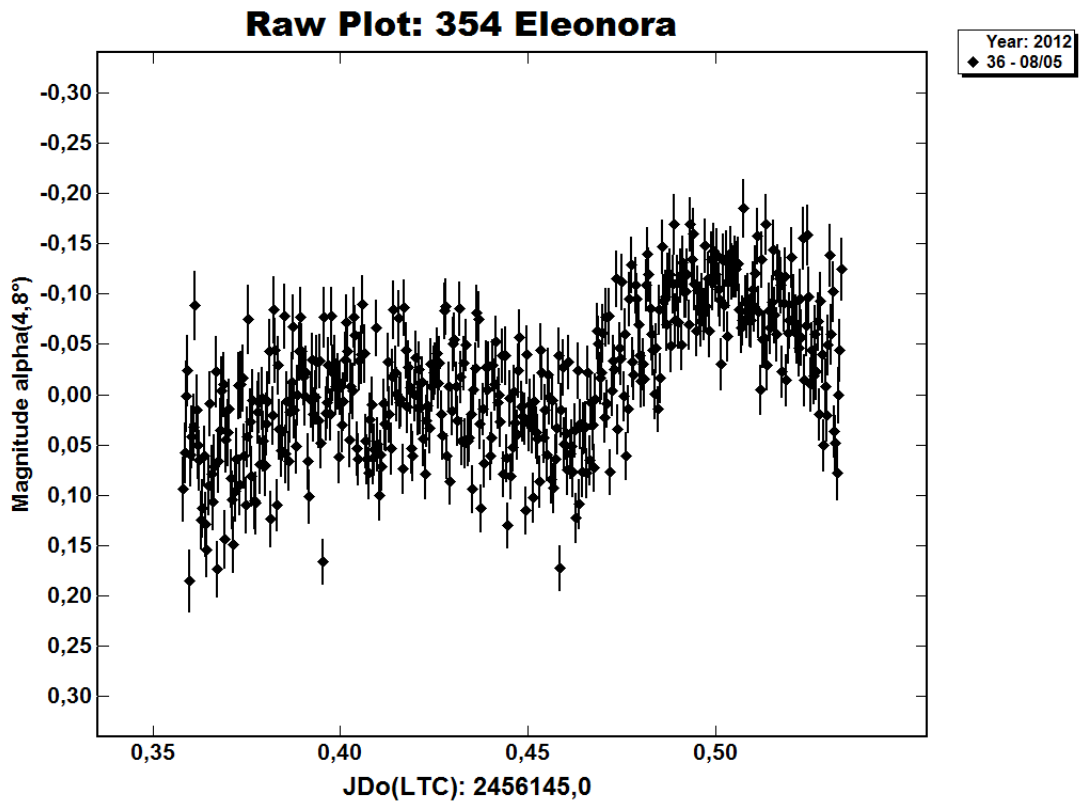


Figure 13: Raw data 2012/08/07

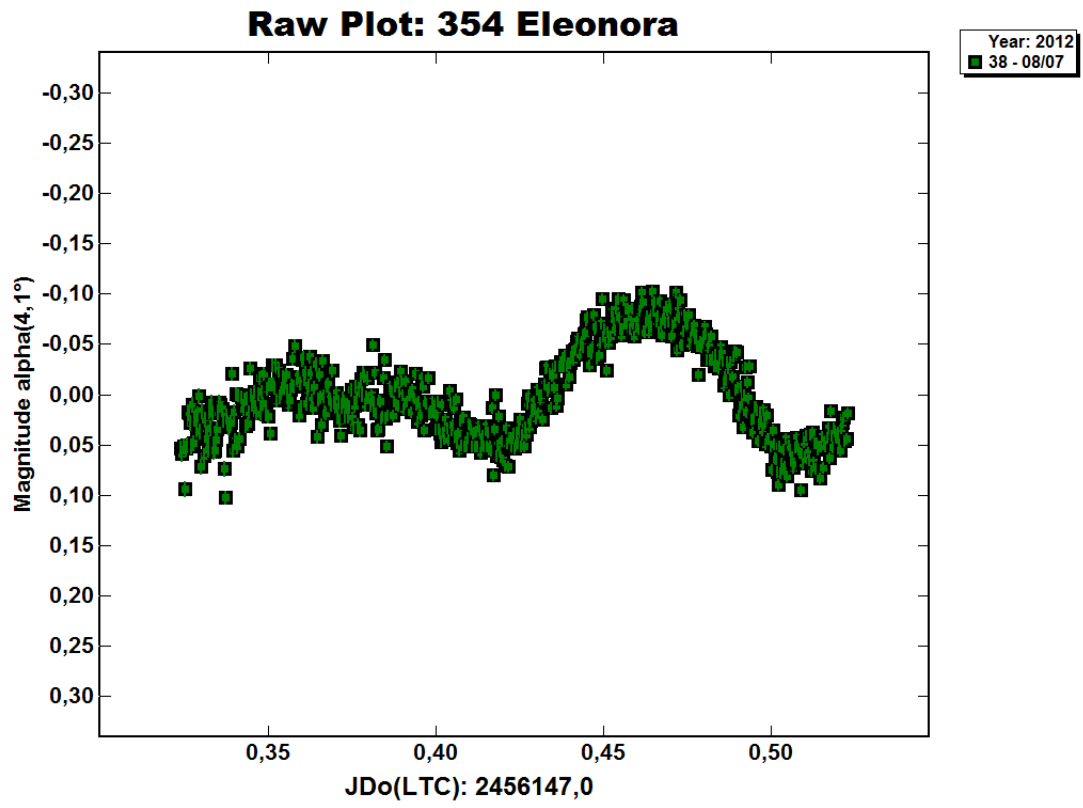
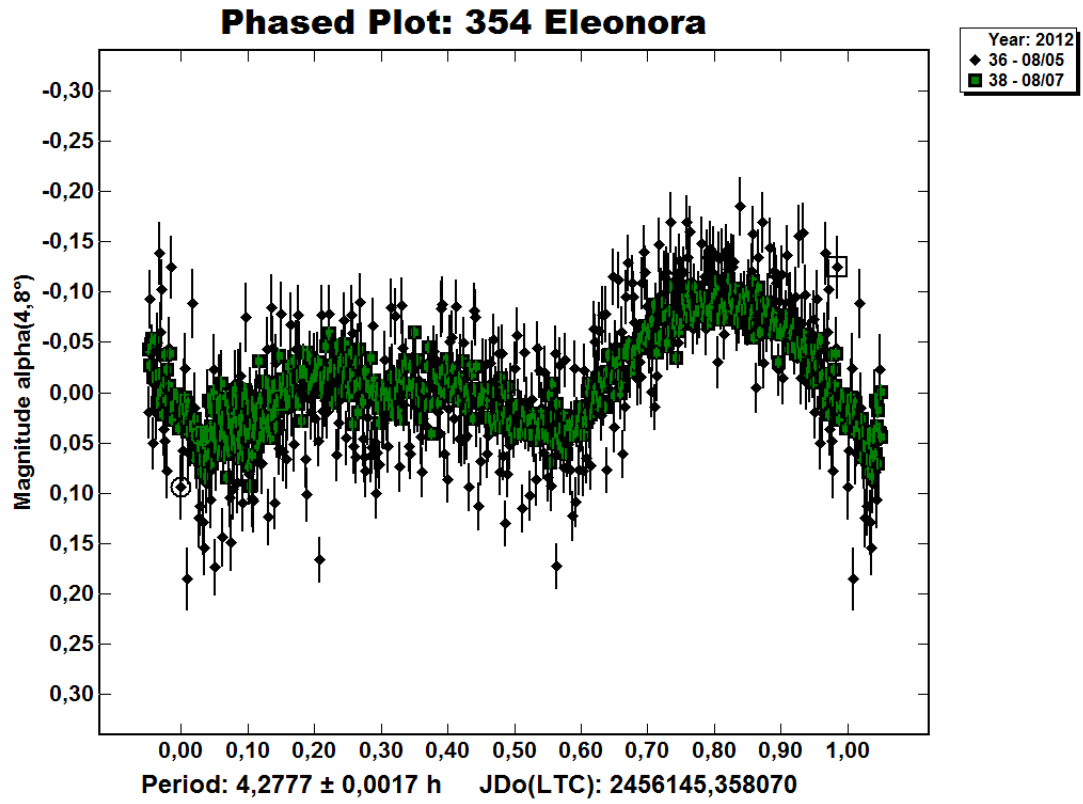


Figure 14: 354 Eleonora lightcurve



## 4.2 79 Eurynome

Table 10: Orbital elements of 79 Eurynome

Element	Value
a	2.44401 AU
e	0.191646
i	4.618 deg
$\Omega$ (node)	206.634 deg
$\omega$ (peri)	200.878 deg
M	125.002 deg
Absolute Magnitude (H)	7.96 mag
Slope parameter (G)	0.25 mag
Perihelion (q)	1.9756 AU
Aphelion (Q)	2.9124 AU
Orbital period	1395.58 days
Diameter	66.47 km
Geometric albedo	0.2618
Rotation period	5.978h

There are two pairs of  $(\lambda, \beta)$  and two shape models for the asteroid 79 Eurynome:

$$\lambda_1 = 54^\circ$$

$$\beta_1 = 24^\circ$$

and

$$\lambda_1 = 228^\circ$$

$$\beta_1 = 30^\circ$$

Figure 15: Shape model of 79 Eurynome (1) (DAMIT)

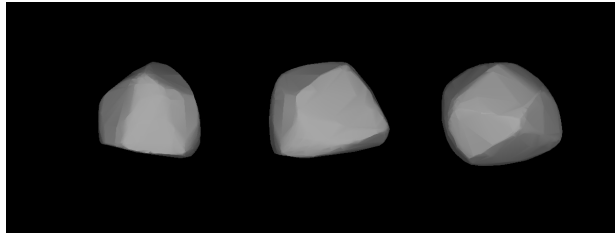
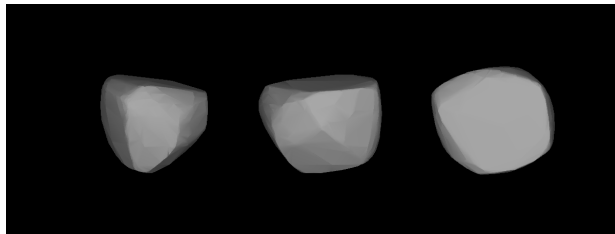


Figure 16: Shape model of 79 Eurynome (2) (DAMIT)



79 Eurynome was discovered by J. C. Watson on September 14, 1863. Eurynome was observed in 1974 (Scaltriti and Zappala 1976; Schober 1976) and in 1983 (Di Martino and Cacciatori 1984; Barucci et al. 1985) during oppositions. It was observed again in 1989 (T. Mickalowski and F.P. Velickho 1990) and its period was found  $P = 5.9777\text{h}$ .

The following asteroid was observed for one night only and its lightcurve is partially covered, thus its rotation period could not be fully obtained. Its orbital elements at Epoch 2456800.5 (2014-May-23.0) (Reference: JPL 87) heliocentric ecliptic J2000 and the lightcurve resulting from the Holomon Astronomical Station data with period  $P = 5.815 \pm 0.001\text{h}$  are shown in the table above and in the following figures.

Figure 17: Raw data 2012/10/01

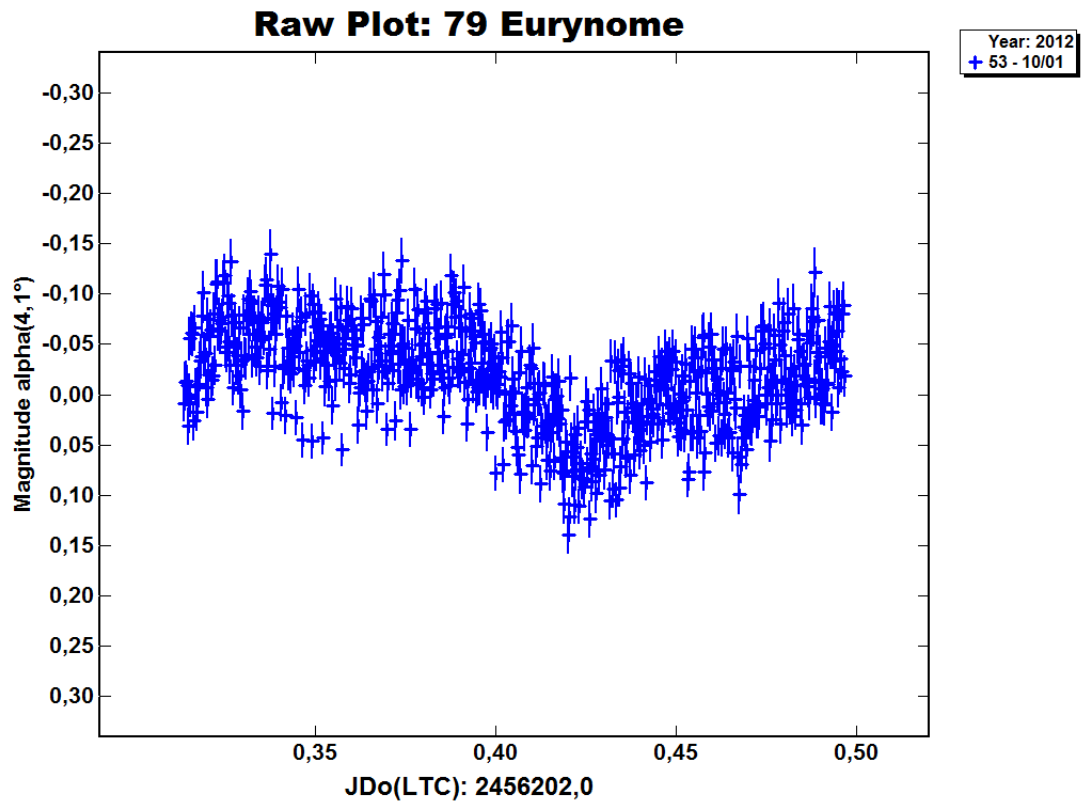
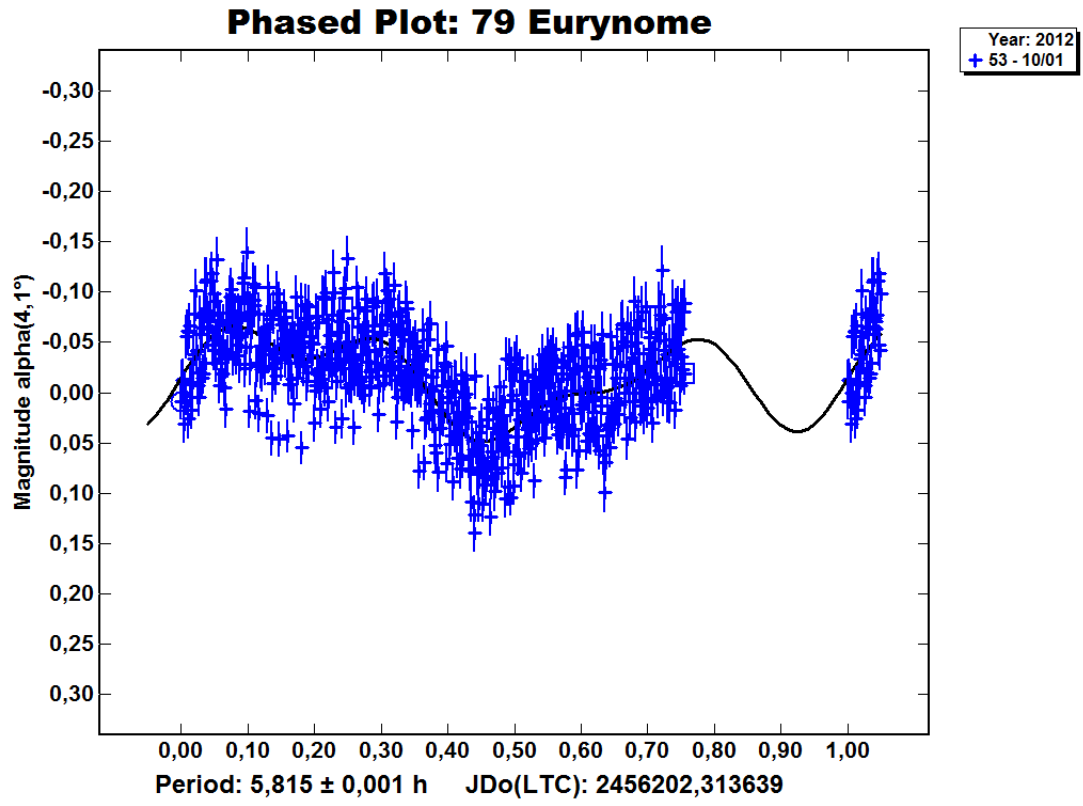


Figure 18: 79 Eurynome lightcurve



### 4.3 213 Lilaea

Table 11: Orbital elements of 213 Lilaea

Element	Value
a	2.75284 AU
e	0.14616
i	6.803 deg
$\Omega$ (node)	122.116 deg
$\omega$ (peri)	162.561 deg
M	26.543 deg
Absolute Magnitude (H)	8.9 mag
Slope parameter (G)	0.15 mag
Perihelion (q)	2.3505 AU
Aphelion (Q)	3.1552 AU
Orbital period	1668.29 days
Diameter	83.01 km
Geometric albedo	0.0897
Rotation period	8.045h

Neither coordinates for spin axis nor shape models for 213 Lilaea have been found yet. 213 Lilaea is a large main belt asteroid. It was discovered by German-American astronomer C. H. F. Peters on February 16, 1880 in Clinton, New York and was named after Lilaea, a Naiad in Greek mythology.

Photometric observations of this asteroid in 1987 (Kenneth W. Zeigler, The Minor Planet Bulletin) gave a lightcurve with a period of  $7.85 \pm 0.003$  hours and a brightness variation of 0.07 in magnitude. In 1995 M. Di Martino et al. found the period  $P = 8.045\text{h}$  with an amplitude  $\text{amp} = 0.20\text{mag}$ . The curve is asymmetrical with two distinct minima.

Although 213 was observed for three nights, the observations did not cover the whole rotation, because some data overlapped which means that the same region of the asteroid was observed. Its orbital elements at Epoch 2456800.5 (2014-May-23.0) (Reference: JPL 76) heliocentric ecliptic J2000 and the lightcurve resulting from the Holomon Astronomical Station data with period  $P = 8.034 \pm 0.004$  are shown in the previous table and in the following figures.

Figure 19: Raw data 2013/04/28

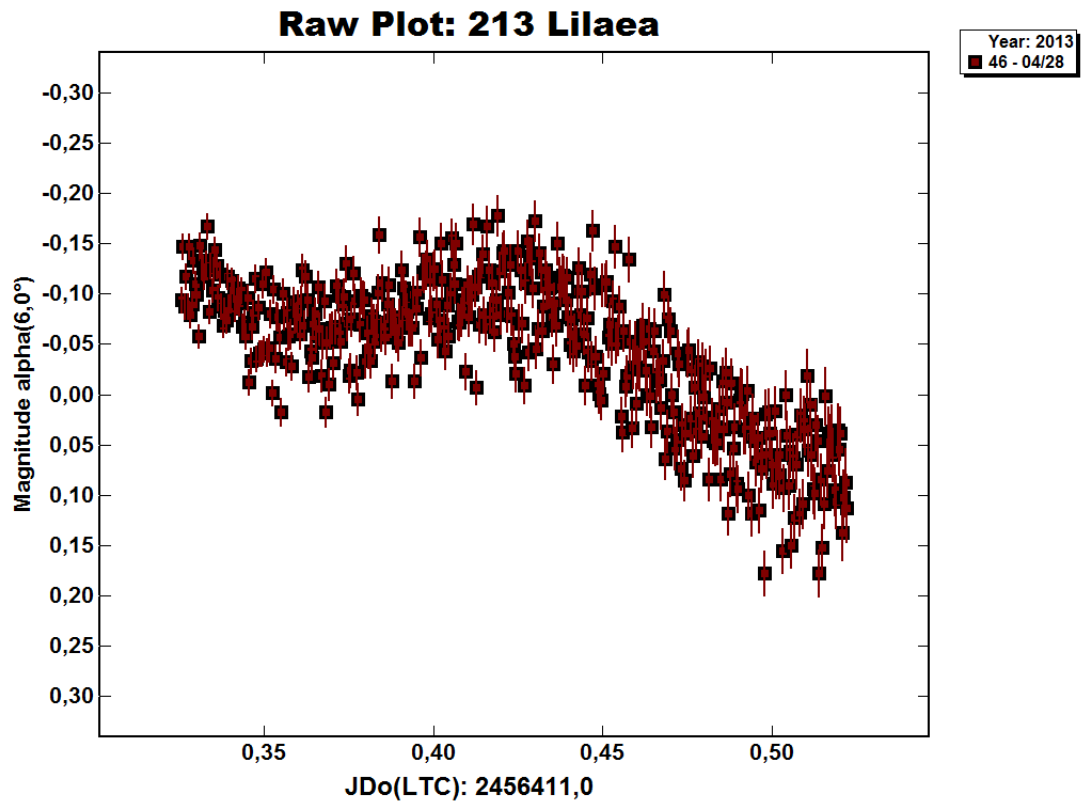


Figure 20: Raw data 2013/04/29

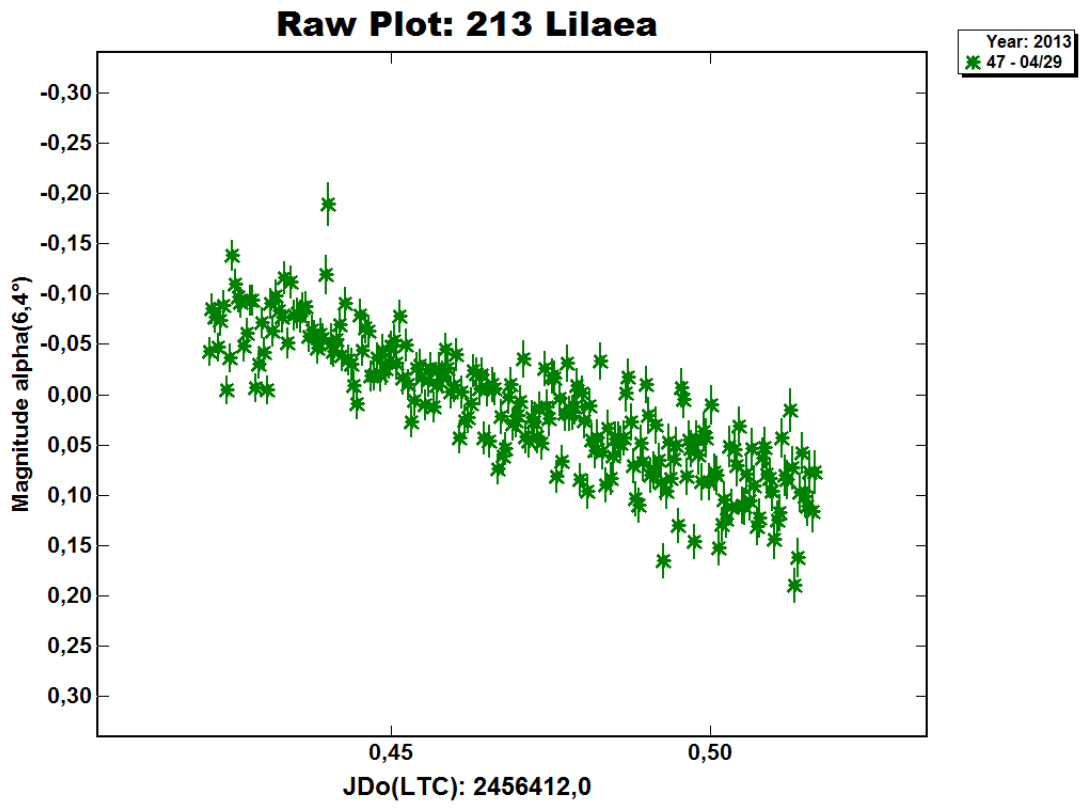


Figure 21: Raw data 2013/05/02

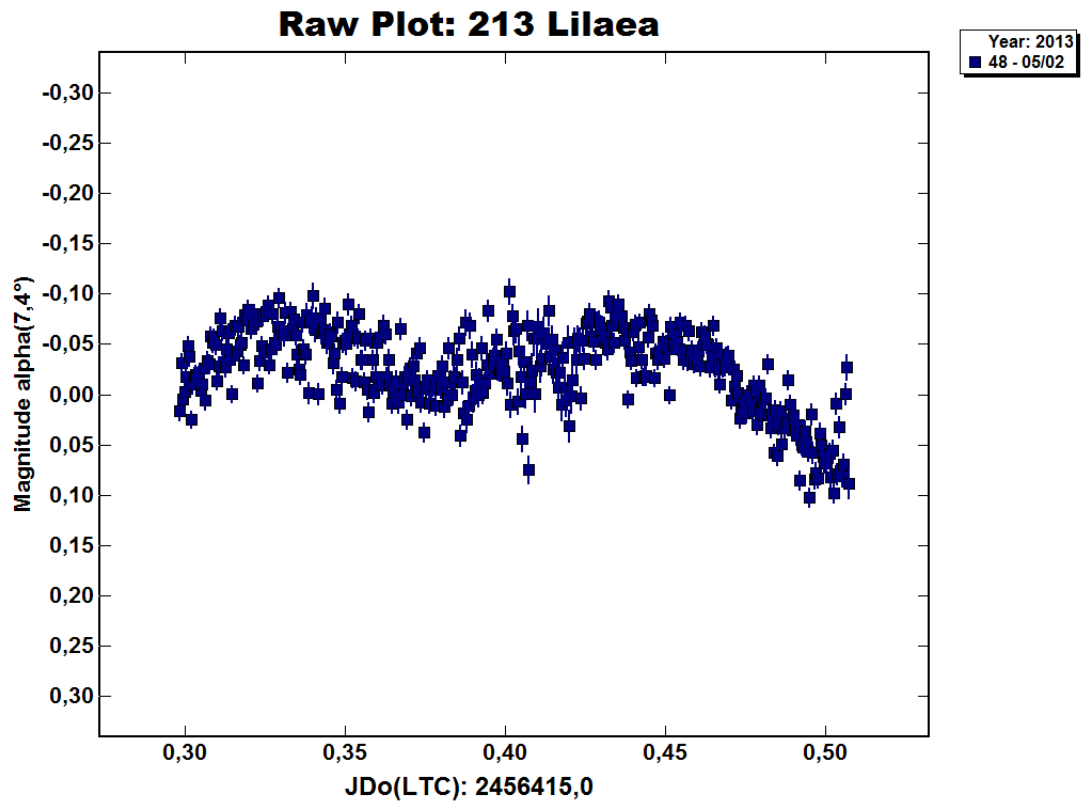
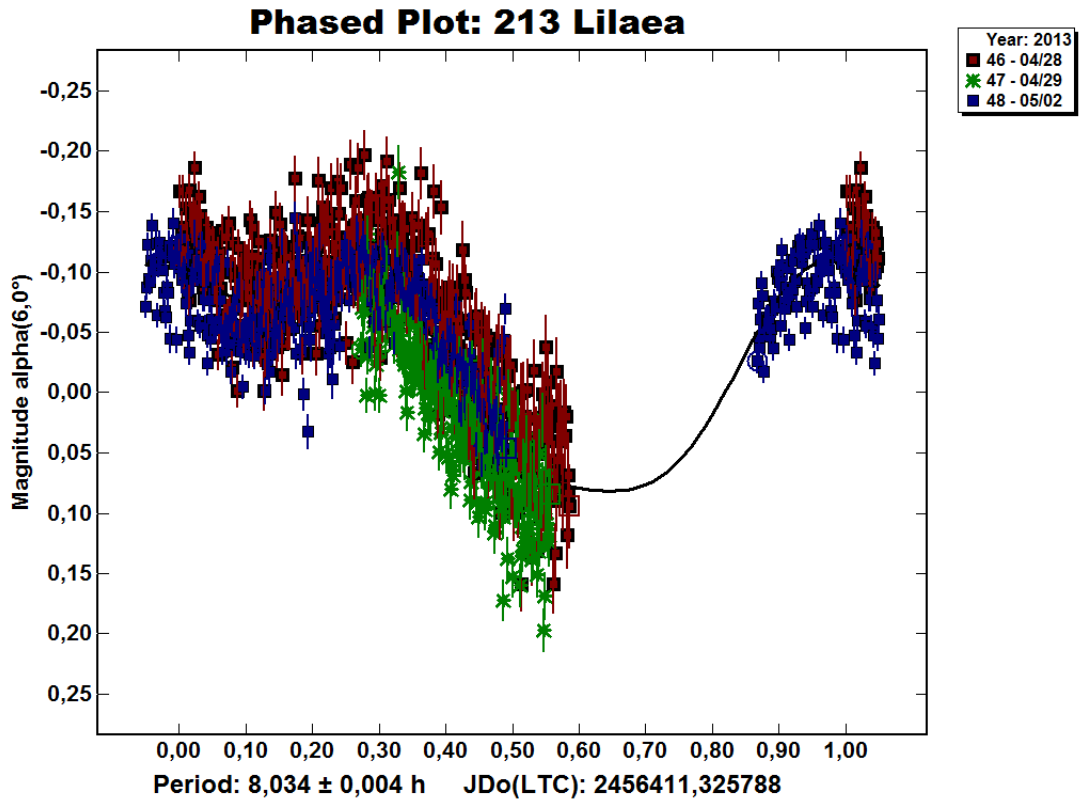


Figure 22: 213 Lilaea lightcurve



## 4.4 374 Burgundia

Table 12: Orbital elements of 374 Burgundia

Element	Value
a	2.77895 AU
e	0.081185
i	8.986 deg
$\Omega$ (node)	219.083 deg
$\omega$ (peri)	25.887 deg
M	124.415 deg
Absolute Magnitude (H)	8.67 mag
Slope parameter (G)	0.15 mag
Perihelion (q)	2.5533 AU
Aphelion (Q)	3.0046 AU
Orbital period	1692.08 days
Diameter	44.67 km
Geometric albedo	0.3014
Rotation period	6.972h

374 Burgundia is a typical main belt asteroid that was discovered by Auguste Charlois on September 18, 1893 in Nice. It was named after the former French region of Burgandy. 374 Burgundia was observed for five nights in August 1999 (Worman, W. E.; Fieber, Sherry; Hulet, Kiernan). The period of rotation is  $6.972 \pm 0.007$  hours, and the lightcurve has an amplitude of  $0.176 \pm 0.011$  magnitude. Its orbital elements at Epoch 2456800.5 (2014-May-23.0) (Reference: JPL 8) heliocentric ecliptic J2000 and the lightcurve resulting from the Holomon Astronomical Station data with period  $P = 6.969 \pm 0.001$ h are shown in the previous table and in the following figures.

Figure 23: Raw data 2013/08/08

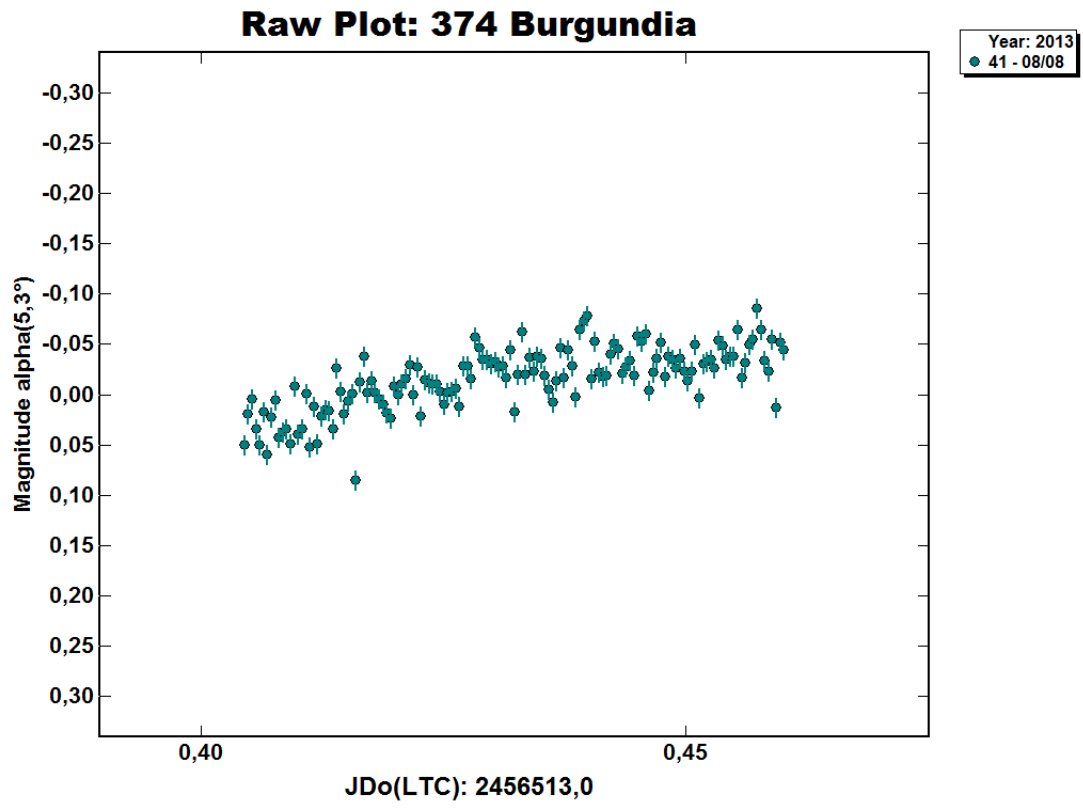


Figure 24: Raw data 2013/08/09

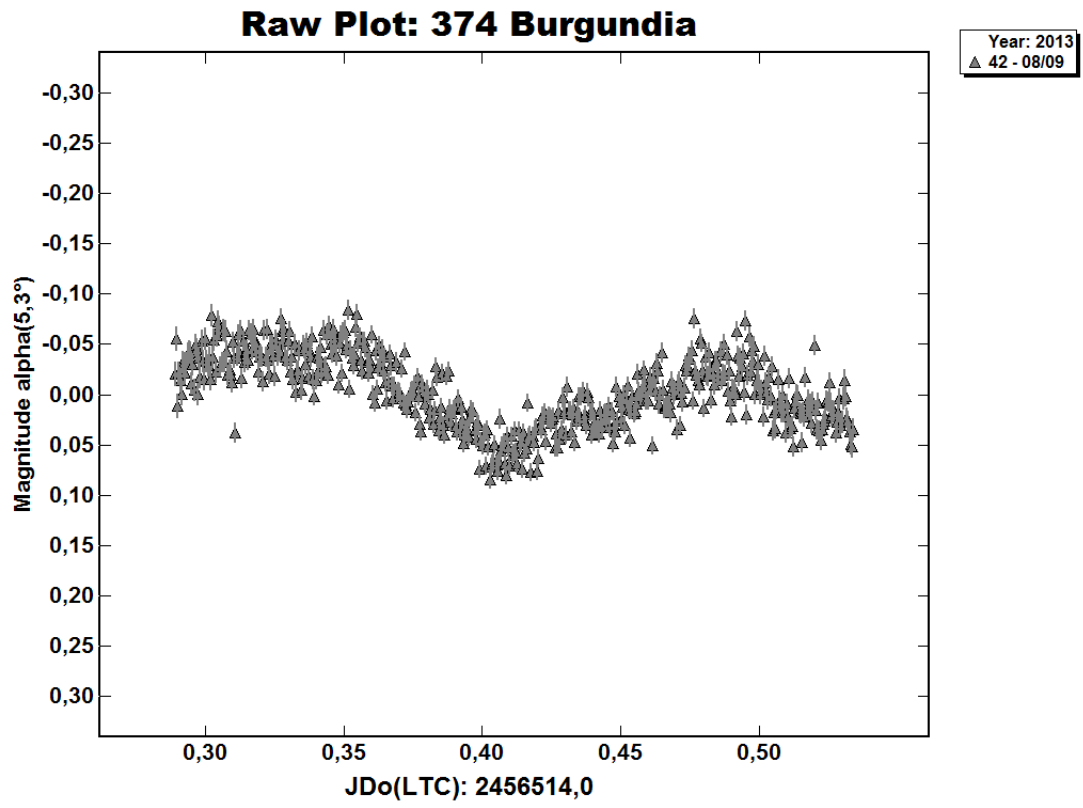


Figure 25: Raw data 2013/08/10a

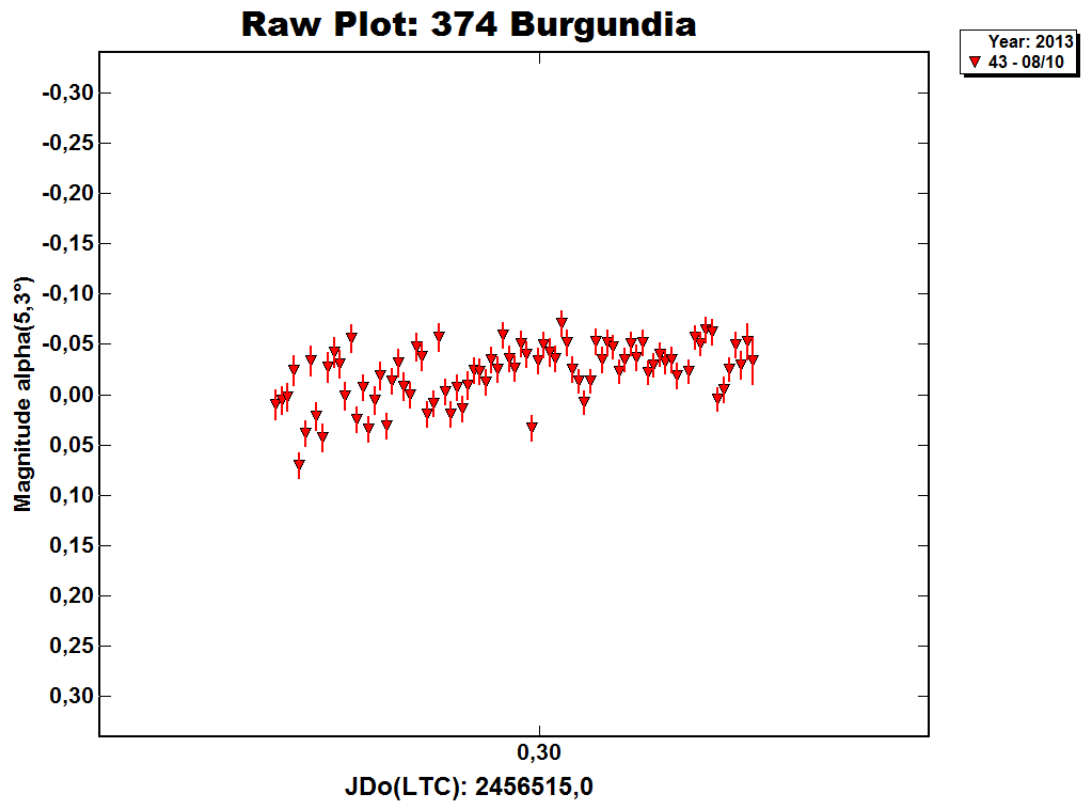


Figure 26: Raw data 2013/08/10b

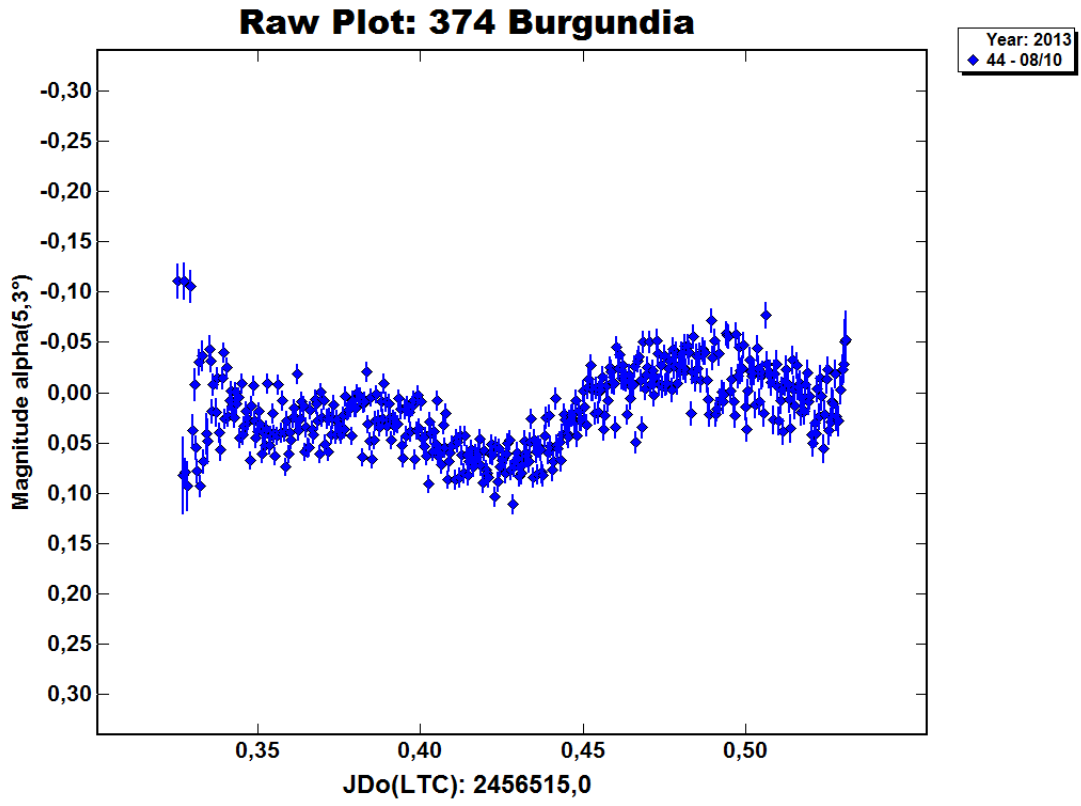
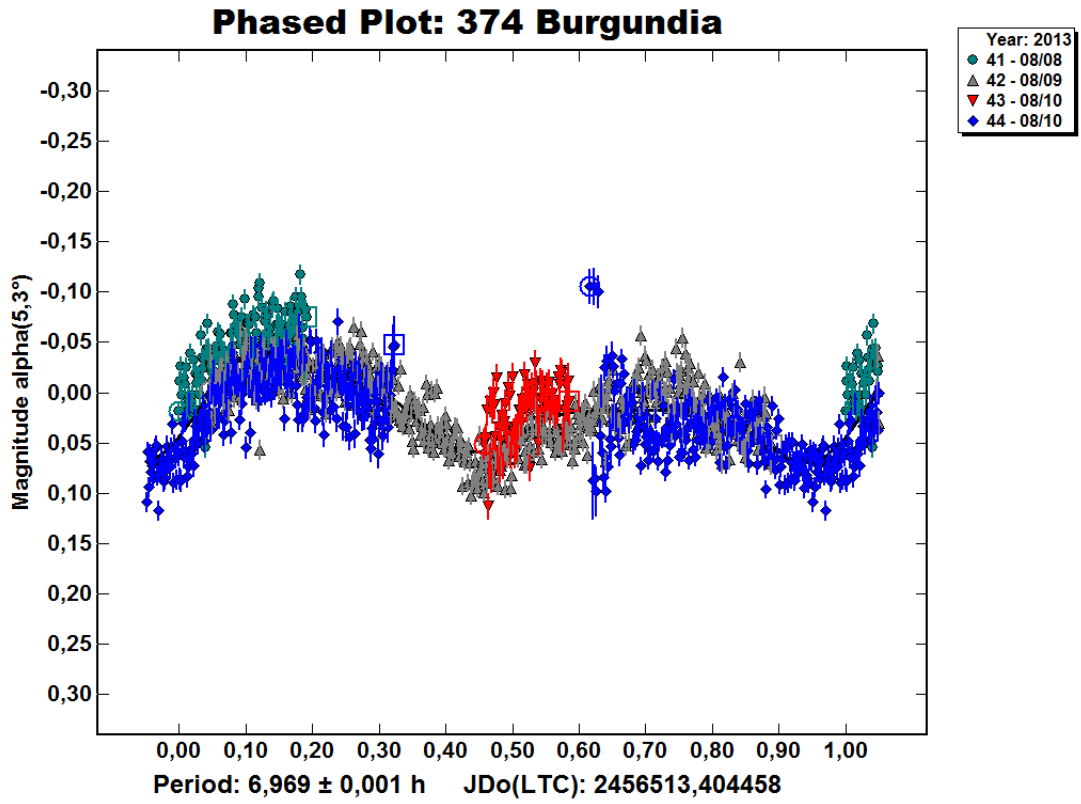


Figure 27: 374 Burgundia lightcurve



## 4.5 173 Ino

Table 13: Orbital elements of 173 Ino

Element	Value
a	2.74366
e	0.206005
i	14.212 deg
$\Omega$ (node)	148.273 deg
$\omega$ (peri)	227.985 deg
M	4.811 deg
Absolute Magnitude (H)	7.66 mag
Slope parameter (G)	0.01 mag
Perihelion (q)	2.1785 AU
Aphelion (Q)	3.3089 AU
Orbital period	1659.95 days
Diameter	154.10 km
Geometric albedo	0.0642
Rotation period	6.163h

173 Ino is a large main-belt asteroid that was discovered by French astronomer Alphonse Borrelly on August 1, 1877, and named after Ino, a queen in Greek mythology. It is a C-type asteroid and has a dark surface and a primitive carbonaceous composition.

The first lightcurve published (Schober 1978) has a rotation period  $P = 5.93 \pm 0.01$ h. Later photometric observations (Debehogne et al. 1990; Erikson 1990) gave periods  $P = 6.15 \pm 0.02$ h and  $P = 6.11 \pm 0.06$ h respectively. Michalowski (1993) found a period of  $P = 6.163$ h, but in 2005 he found  $P = 6.11651$ h. Observations in 2004 (D. Gandolfi, C. Blanco, M. Cigna) gave a period  $P = 6.111 \pm 0.002$ h and amplitude  $\text{amp} = 0.14$ mag. The combined data gave an irregular, asymmetrical light curve with a period of  $6.163 \pm 0.005$  hours and a brightness variation of 0.10–0.15 in magnitude. The asteroid is rotating in a retrograde direction. Its orbital elements at Epoch 2456800.5 (2014-May-23.0) (Reference: JPL 64) heliocentric ecliptic J2000 and the lightcurve resulting from the Holomon Astronomical Station data with period  $P = 6.111 \pm 0.005$ h are shown in the previous table and in the following figures.

4.5.1 173 Ino  $phase = 20^\circ.8$

Figure 28: Raw data 2013/04/29

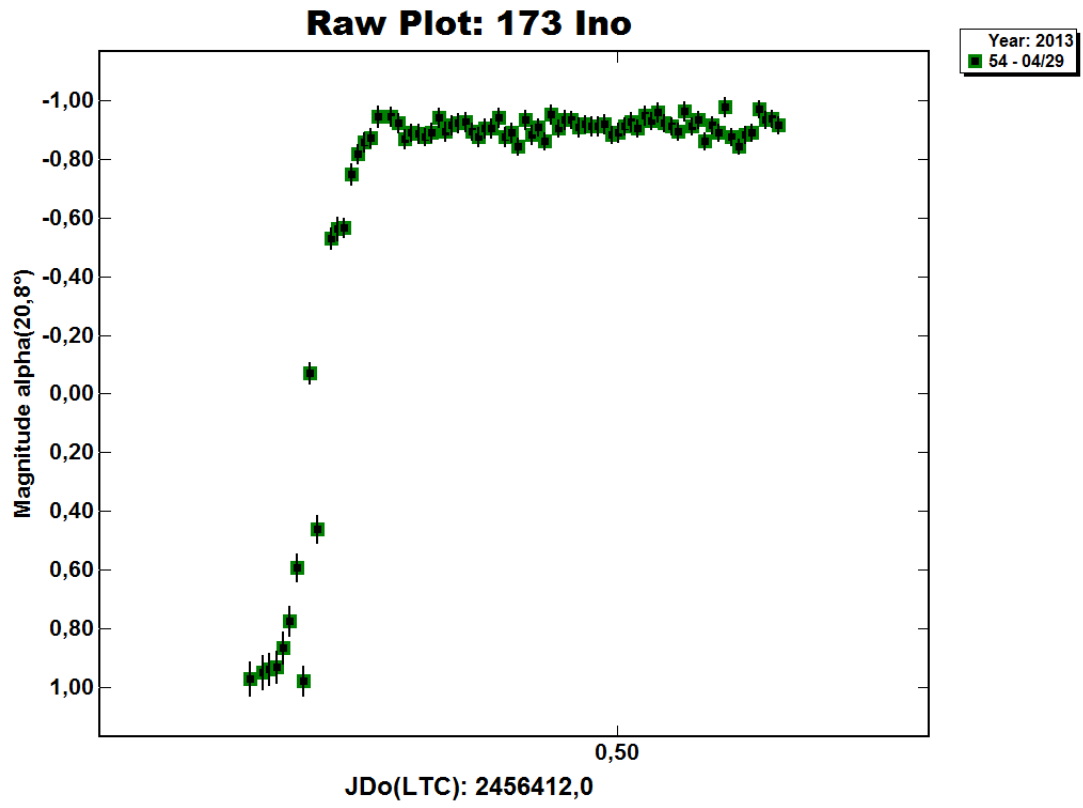


Figure 29: Raw data 2013/05/02

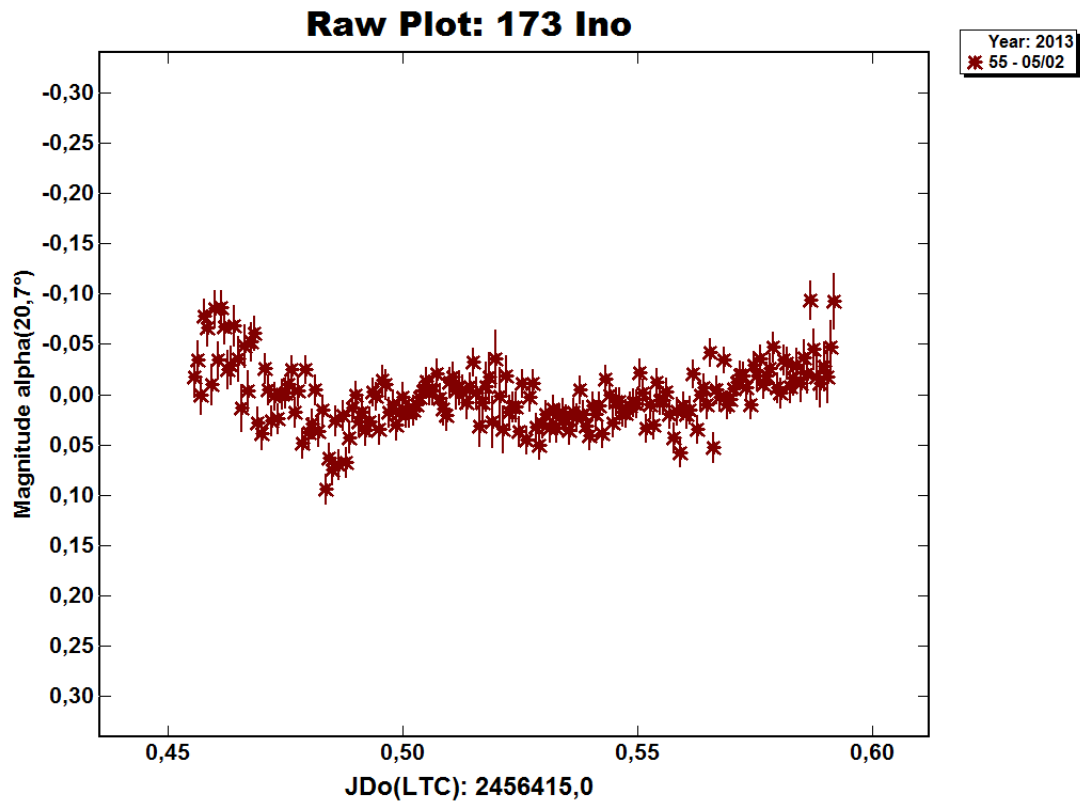


Figure 30: Raw data 2013/05/04

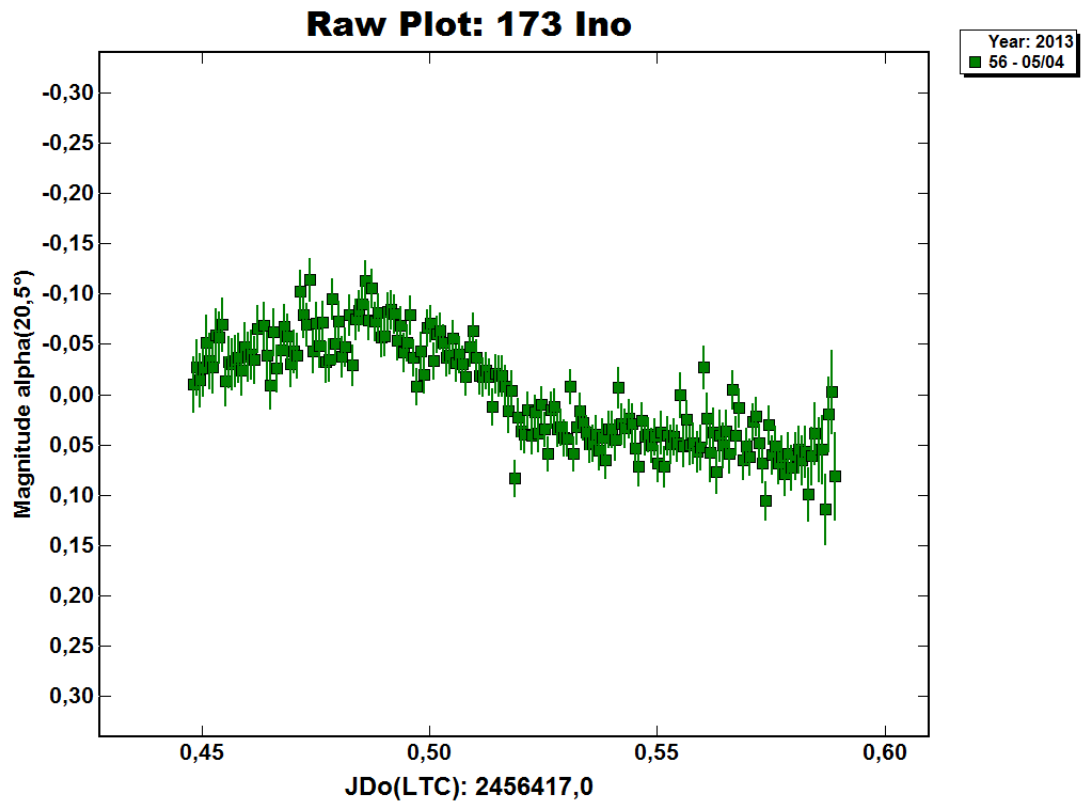
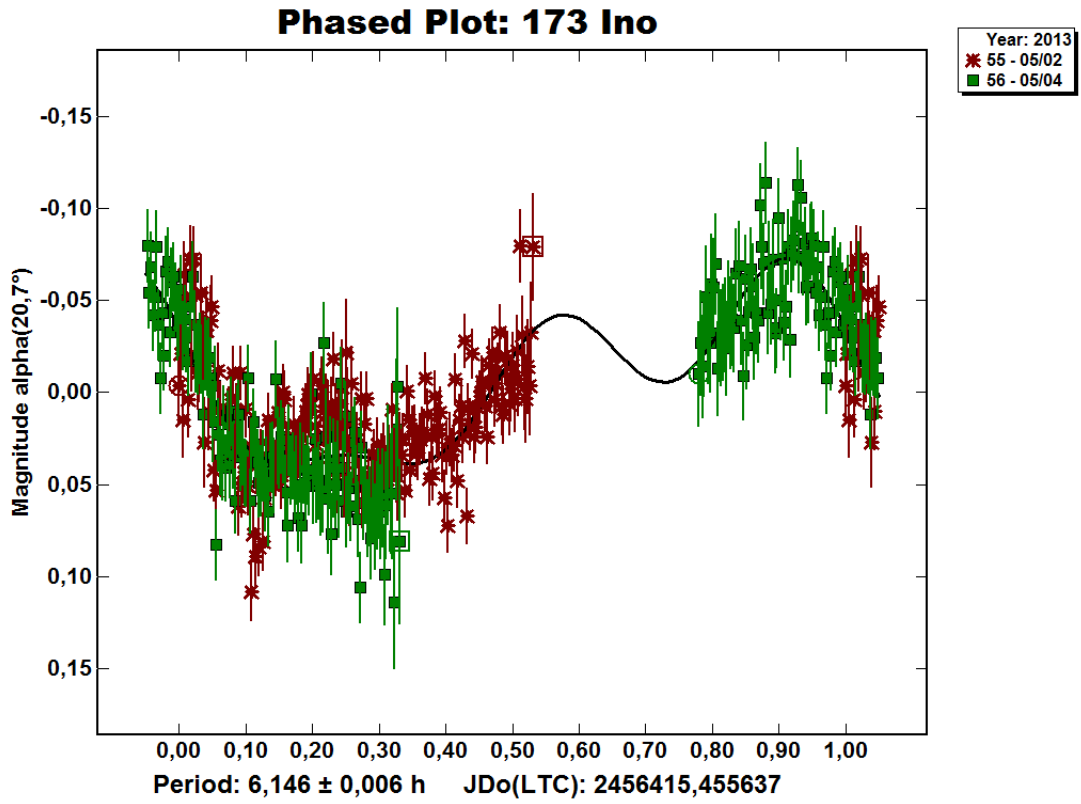


Figure 31: 173 Ino lightcurve (ph.)



#### 4.5.2 173 Ino near opposition

Figure 32: Raw data 2013/07/25

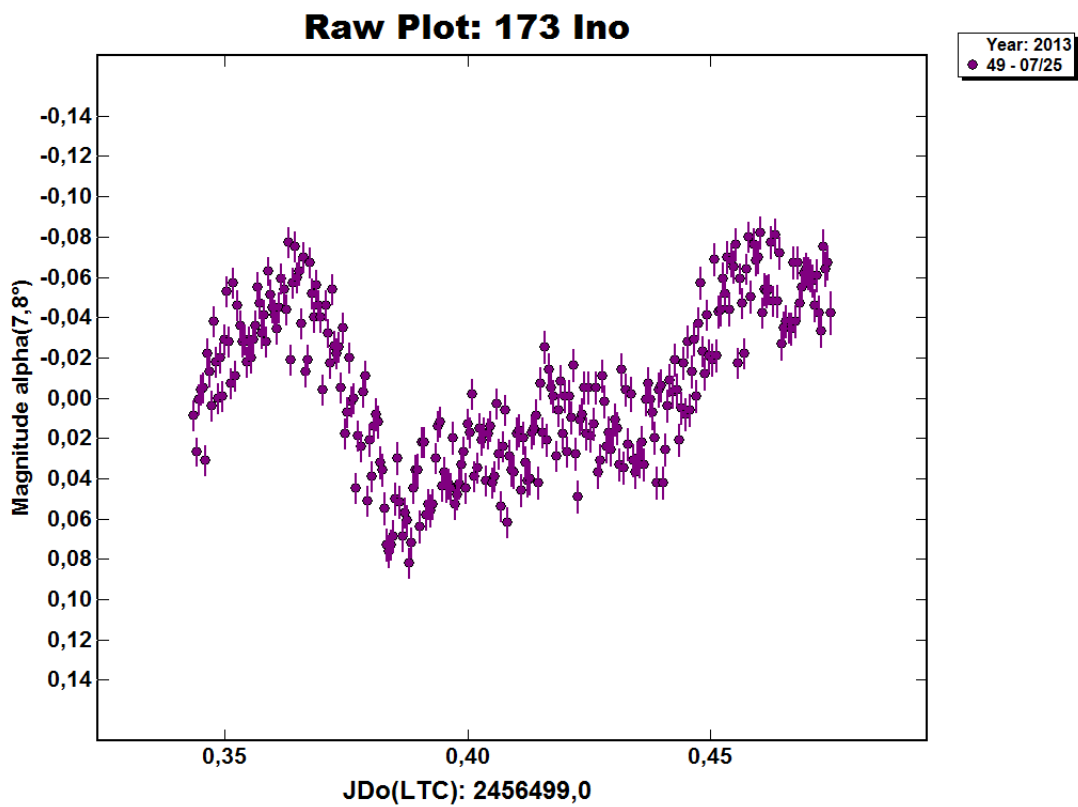


Figure 33: Raw data 2013/07/26

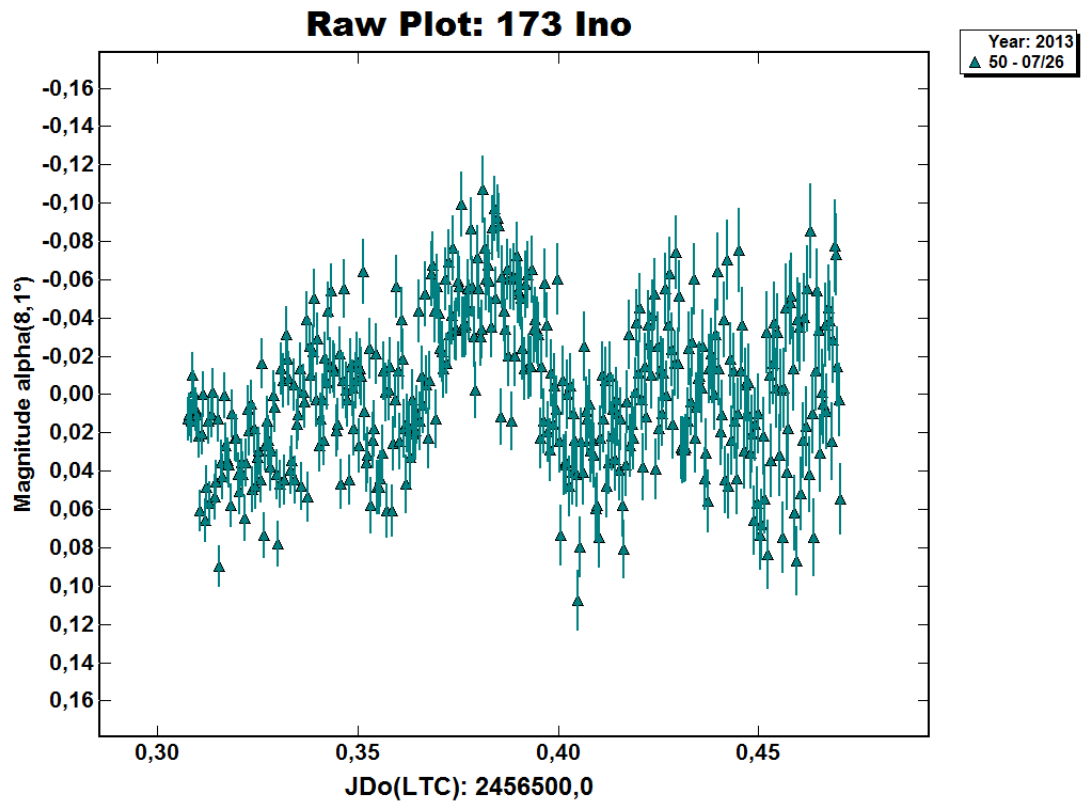


Figure 34: Raw data 2013/07/27

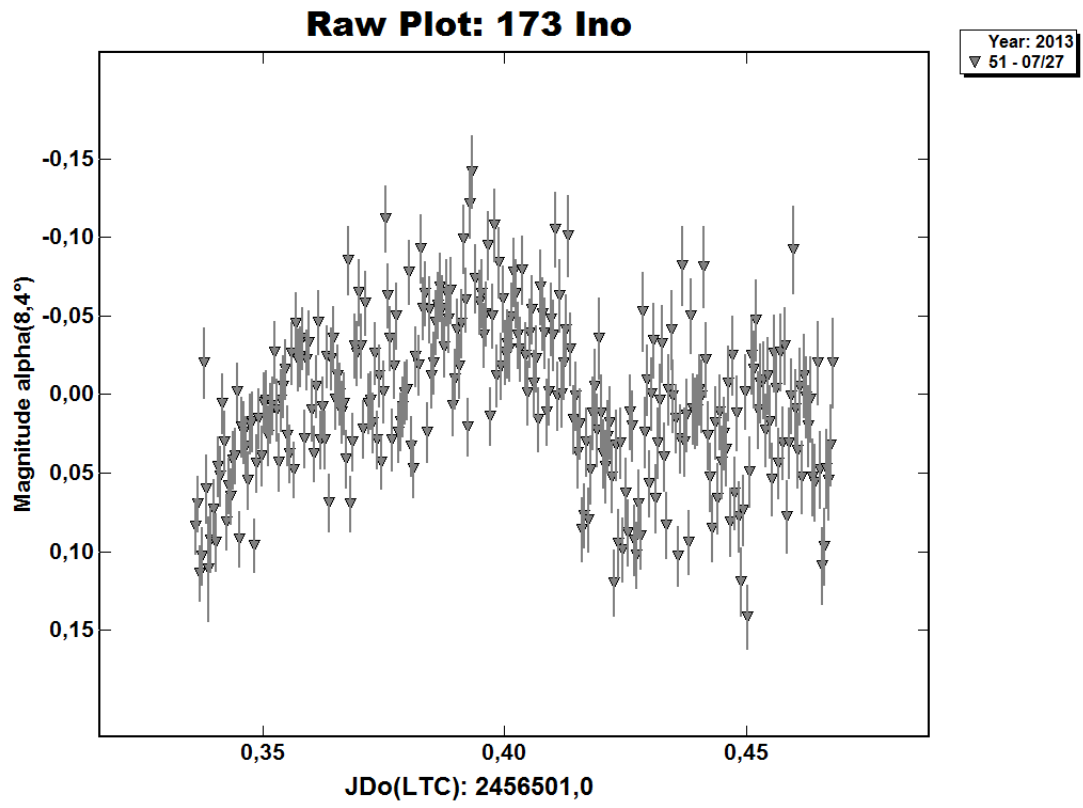


Figure 35: Raw data 2013/07/28

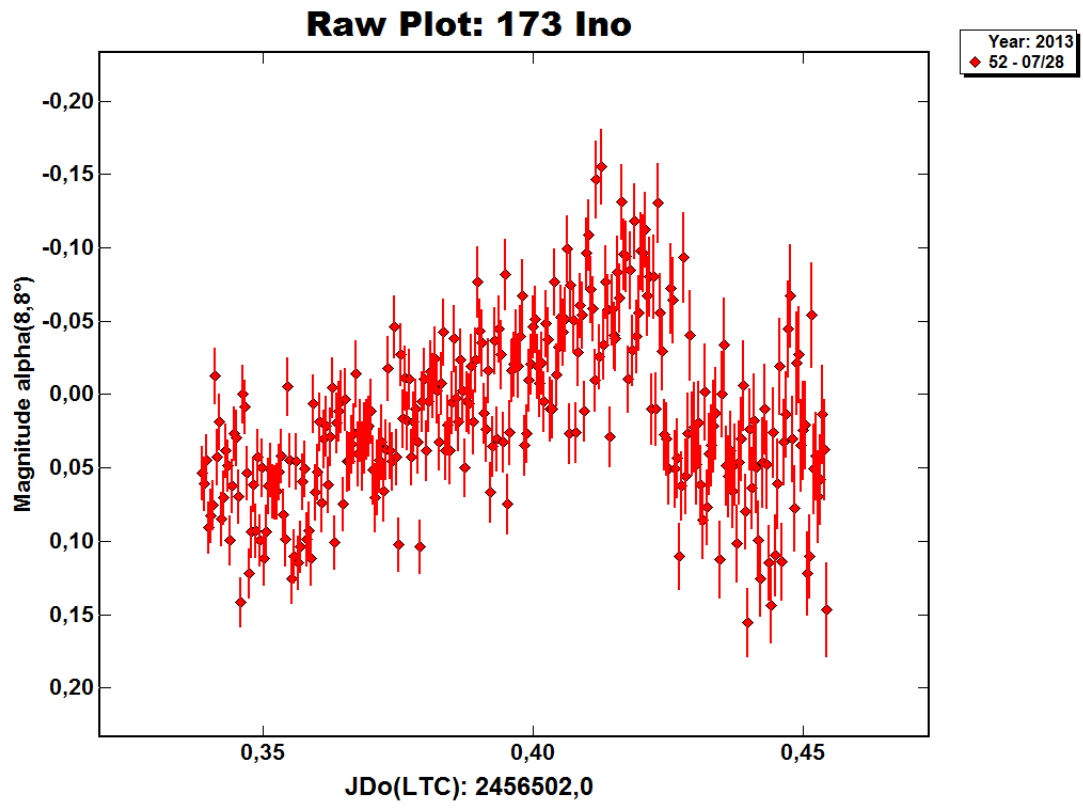
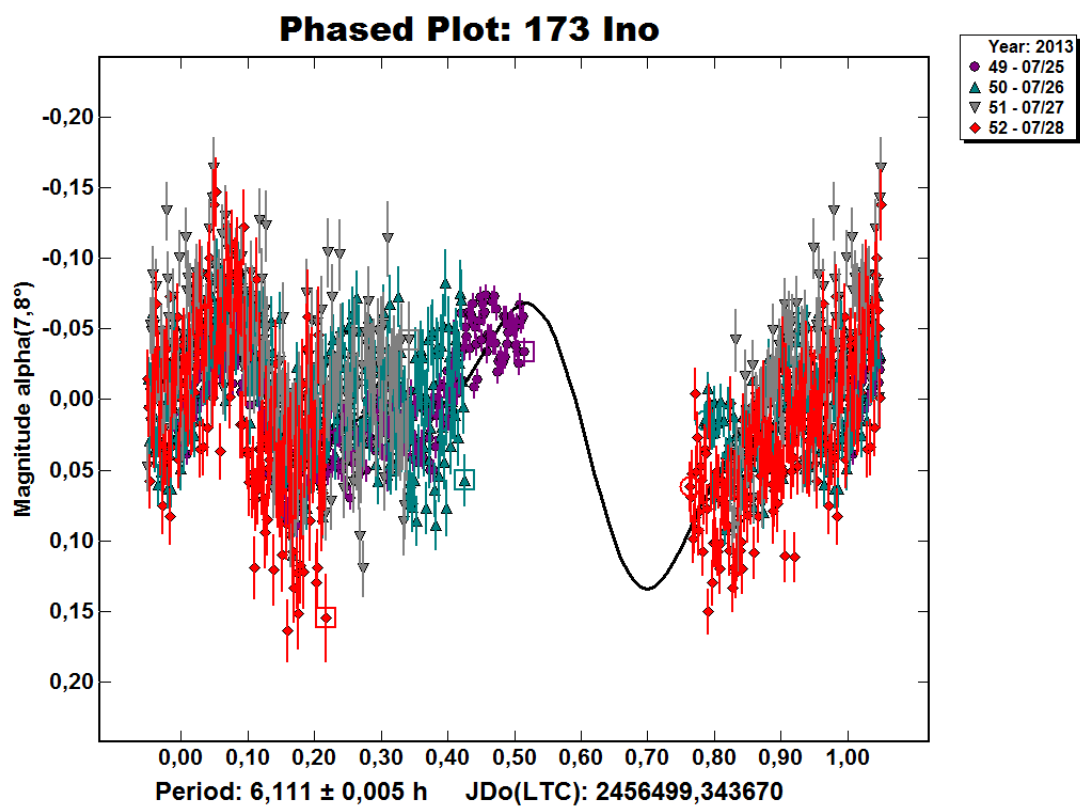


Figure 36: 173 Ino lightcurve (opp.)



## 5 Conclusions

354 Eleonora has a short rotation period, hence a great part of its period was observed on the first night and the whole period on the second night. A complete lightcurve was created by using data from two nights only. The resulting period agree completely with the previous reported period,  $P = 4.277 \pm 0.0017\text{h}$  with an amplitude  $\text{amp} = 0.17\text{mag}$ .

79 Eurynome was observed for one night only, thus the whole period could not be covered by the observations. However, an attempt for a calculation of the period was made and the deviation was not very large.

213 Lilaea was observed for six consecutive nights, but only the data from three nights were usable due to weather difficulties. These three nights were not enough to cover the whole period, because its period is longer than the two previous asteroids and because a lot of the data happened to overlap which means that the same regions of the asteroid surface were observed. The period calculated is  $P = 8.034 \pm 0.004\text{h}$  with amplitude  $\text{amp} = 0.26$ .

374 Burgundia was observed for three nights and its whole period was covered:  $P = 6.969 \pm 0.001\text{h}$  with  $\text{amp} = 0.18\text{mag}$  which is very close to the previous reported period  $P = 6.972\text{h}$ .

Finally, 173 Ino was observed for 7 nights. Three of them were on 29/4, 02/05 and 04/05 and its phase was 20.7 degrees. Data from 29/04 could not be used for the composite lightcurve because there was an occultation as it can be seen on Fig. 28. The period calculated from the other two nights is  $P = 6.146 \pm 0.006\text{h}$ . The rest 4 nights were 25/7-28/7 with an approximate phase 7.8 degrees and the period calculated is  $P = 6.111 \pm 0.005\text{h}$  with  $\text{amp} = 0.26$ . Although the whole period was not covered because of the overlapping data, its value is quite close to previously reported.

Table 14: Studied asteroids

Asteroid	Previously reported period (hr)	Results from HAS
79 Eurynome	5.978	$5.815 \pm 0.001$
173 Ino (near opp)	6.111	$6.111 \pm 0.005$
213 Lilaea	8.045	$8.034 \pm 0.004$
354 Eleonora	4.277	$4.277 \pm 0.0017$
374 Burgundia	6.972	$6.969 \pm 0.001$

## References

- Astropedia by Astropedia/Chris Impey, Teach Astronomy, Origin of Meteorites  
URL: <http://m.teachastronomy.com/astropedia/article/Origin-of-Meteorites>
- Bendjoya Ph., Zappalà V. *Asteroid Family Identification*
- Binary asteroid, URL: [http://en.wikipedia.org/wiki/Binary\\_asteroid](http://en.wikipedia.org/wiki/Binary_asteroid)
- Bottke Jr. W. F., Cellino A., Paolicchi P., Binzel R. P. *An Overview of the Asteroids: The Asteroids III perspective*, 2002
- Bowell E., Oszkiewicz D.A., Wasserman L.H., Muinonen K., Penttilä A., Trilling D.E. *Asteroid spin-axis longitudes from the Lowell Observatory database*
- Canadian Space Agency, Satellites, URL: <http://www.asc-csa.gc.ca/eng/satellites/neosnat/>
- Cole G.H.A. , Woolfson M.M. *Planetary science, the science of planets around stars*, Institute of Physics Publishing Bristol and Philadelphia, 2002
- DAMIT, Database of Asteroid Models from Inversion Techniques,  
URL: [http://astro.troja.mff.cuni.cz/projects/asteroids3D/web.php?page=project\\_main\\_page](http://astro.troja.mff.cuni.cz/projects/asteroids3D/web.php?page=project_main_page)
- DAMIT, Database of Asteroid Models from Inversion Techniques, Database – Description Light curve inversion  
URL: [http://astro.troja.mff.cuni.cz/projects/asteroids3D/web.php?page=db\\_description](http://astro.troja.mff.cuni.cz/projects/asteroids3D/web.php?page=db_description)
- Durech J., Sidorin V., Kaasalainen M. *DAMIT: a database of asteroid models*
- Dymock R. *Asteroids and dwarf planets and how to observe them*, 2010  
Springer Science+Business Media

- ESA, Universita di Pisa, SpaceDys, Astronomical Observatory of Belgrade  
*AstDys-2, Asteroids-Dynamics site*  
URL: <http://hamilton.dm.unipi.it/astdys2/index.php?pc=5>
- ESA, Science and Technology, Space missions to asteroids  
URL: <http://sci.esa.int/home/2306-space-missions-to-asteroids/>
- ESA, Space Science, Asteroids: Families of asteroids  
URL: [http://www.esa.int/Our\\_Activities/Space\\_Science/Asteroids\\_Families\\_of\\_asteroids](http://www.esa.int/Our_Activities/Space_Science/Asteroids_Families_of_asteroids)
- ESA, Space Science, Asteroids: Structure and Composition of asteroids  
URL: [http://www.esa.int/Our\\_Activities/Space\\_Science/Asteroids\\_Structure\\_and\\_composition\\_of\\_asteroids](http://www.esa.int/Our_Activities/Space_Science/Asteroids_Structure_and_composition_of_asteroids)
- Gandolfi D., Blanco C., Cigna M. *Asteroid photometric observations at Catania and Padova Observatories*, 2005
- Hestroffer D., dell'Oro A., Cellino A., Tanga P. *The Gaia Mission and the Asteroids. A perspective from space astrometry and photometry for asteroids studies and science.*
- Howel S.B. *Handbook of CCD astronomy*, second edition, Cambridge
- IAU, International Astronomical Union,  
URL: <http://www.iau.org/news/pressreleases/detail/iau0601/>
- IAU, Minor Planet Center, Minor Planet Lightcurve Parameters  
URL: <http://www.minorplanetcenter.net/iau/lists/LightcurveDat.html>
- Licchelli D. *Rotation period and lightcurve analysis of selected asteroids*, 2007
- Masiero J., Jedicke R., Durech J., Gwyn S., Denneau L., Larsen J. *The Thousand Asteroid Light Curve Survey*
- Minor Planet Bulletin, URL: <http://www.minorplanet.info/mpbdownloads.html>
- MPO Users Guide, 1993-2010 Bdw Publishing

- Murray C.D. and Dermott S.F. *Solar System Dynamics*, Cambridge University Press, 1999
- NASA, Jet Propulsion Laboratory, California Institute of Technology, Asteroids URL: <http://ssd.jpl.nasa.gov/?asteroids>
- NASA, Jet Propulsion Laboratory, California Institute of Technology, Asteroid Watch,  
URL: <http://www.jpl.nasa.gov/asteroidwatch/>
- NASA, Jet Propulsion Laboratory, California Institute of Technology, Solar System Exploration  
URL: <http://solarsystem.nasa.gov/planets/profile.cfm?Object=Asteroids&Display=OverviewLong>
- NASA, Missions, URL: [http://www.nasa.gov/mission\\_pages/dawn/main/index.html#.U7vZRh\\_FsUR](http://www.nasa.gov/mission_pages/dawn/main/index.html#.U7vZRh_FsUR)
- NASA, National Aeronautics and space administration, Near Earth Object Program  
URL: <http://neo.jpl.nasa.gov/glossary/h.html>
- Ostro S.J., Asteroid Radar Research  
URL: <http://echo.jpl.nasa.gov/introduction.html>
- Polishook D. - Tel-Aviv University, Spin Evolution Mechanisms of Asteroids  
URL: <http://wise-obs.tau.ac.il/~david/OnSpinEvolution.htm>
- Polishook D., Brosch N. *Photometry and Spin Rate Distribution of Small-Sized Main Belt Asteroids*
- Prado M.E., PERMANENT, Projects to Employ Resources of the Moon and Asteroids Near Earth in the Near Term,  
Meteorites – Samples of Asteroids, Origins of meteorites  
URL: <http://www.permanent.com/meteorites-origins.html>

- Prado M.E., PERMANENT, Projects to Employ Resources of the Moon and Asteroids Near Earth in the Near Term,  
 Meteorite classifications and compositions,  
 URL: <http://www.permanent.com/meteorite-compositions.html>
- Pravec P., Harris A.W., Michalowski T. *Asteroid Rotations*
- Redd N.T., SPACE.com Contributor, June 2012  
 URL: <http://www.space.com/16105-asteroid-belt.html>
- Torppa J. *Lightcurve inversion for asteroid spins and shapes*, 2007
- UCLA, Department of Earth, Planetary and Space Sciences, Department of physics and Astronomy, Introduction to asteroid radar astronomy  
 URL: <http://mel.ess.ucla.edu/jlm/research/NEAs/intro.html>
- Vokrouhlicky D. and Bottke W.F. (2012), Scholarpedia  
 URL: [http://www.scholarpedia.org/article/Yarkovsky\\_and\\_YORP\\_effects](http://www.scholarpedia.org/article/Yarkovsky_and_YORP_effects)
- Warner B.D. *A practical guide to lightcurve photometry and analysis*, 2006  
 Springer Science+Business Media, Inc.
- Warner B.D. *MPO Canopus and PhotoRed Reference Guide*, 1999-2011 Bdw Publishing
- Yarkovsky effect, URL: [http://en.wikipedia.org/wiki/Yarkovsky\\_effect](http://en.wikipedia.org/wiki/Yarkovsky_effect)
- Zappala V., Van Houten-Groeneveld I., and Van Houten C.J. *Rotation period and phase curve of the asteroids 349 Dembowska and 354 Eleonora*, 1979, Astron. Astrophys. Suppl.35, 213-221